Annual report

Modeling, Monitoring and Fault Diagnosis of Spacecraft Air Contaminants

NASA Grant No. NACW-4585

W. Fred Ramirez, Mikhail Skliar, Anand Narayan
Department of Chemical Engineering
University of Colorado
Boulder, Colorado 80309-0424

George W. Morgenthaler, Gerald J. Smith
Department of Aerospace Engineering Sciences,
University of Colorado
Boulder, Colorado 80309-0429

Contents

Chapter 1

Introduction

Safe air is a most vital environmental resource. Its quality is especially critical in an enclosed environment such as spacecraft, submarine, airliner cabin. The importance of the closely related issue of the indoor (workplace) air quality has been repeatedly emphasised in the last twenty years (Berglund et al., 1986; Berglund et al., 1989). It is known (Mølhave et al., 1986) that only a slight degree of air contamination can have an acute health and performance impact on humans.

In addition to background contamination, resulted from material offgassing, microbial growth and normal human activities (James and Coleman, 1994), there is a risk of an accidental contamination release. In the case of spacecraft and other inclosed environments an unexpected event can lead to mission failure or even incapacitation and death since there may be a significant time lag before personnel evacuation becomes possible. An early detection of the contamination event can provide the critical time necessary to take mitigating actions, or to arrange for safe evacuation.

Recent history of space exploration presents some examples of the possible sources of the accidental air contamination (James et al., 1994). One such source is thermodegradation of electronic components in flight hardware (Todd et al., 1993; Todd et al., 1994). It was reported that during Space Shuttle flight STS–28 0.1 grams of polytetrafluoroethylene (PTFE, or Teflon by its trademark), used as a wiring isolation was pyrolyzed within 1.5 seconds. The crew experienced no adverse health effect.

However, it was subsequently estimated that a pyrolysis of 2 grams of PTFE would have affected health and performance of the crew.

Another example of accidental contamination is the fire extinguishant (CO_2) release due to a containment failure, and microbial growth resulting in the release of volatile pollutants into air (Coleman and James, 1994). Based on the experience with the Shuttle, it is estimated that minor contamination events will occur with a frequency of once in 30 days, and moderate accidents (those causing symptoms in the crew) will occur once per year. Details are not available on the accidental releases into Russian spacecraft. However, it is known that air contamination problems have nearly ended a mission (Covault, 1983) and that formaldehyde exposures are a concern (Peto, 1981).

Currently utilized spacecraft air revitalization systems are designed to maintain equilibrium concentrations of contaminants within limits prescribed by spacecraft maximum allowable concentrations (SMACs) (National Research Council, 1994 and 1992). The monitoring of the Space Shuttle air is done off-line, and involves sampling of the spacecraft air immediately before launch and late in the mission (James *et al.*, 1994), with additional samples taken if crew suspects a contamination problem, and subsequent analysis after spacecraft landing. The analysis of taken samples shows that air quality is consistently within the target region. At the same time, this monitoring technique failed to reflect some know contamination problems (such as abovementioned PTFE thermodegradation), or provided inconclusive results. It is also insensitive to the temporal and spatial variations in contaminant concentrations. At the same time, it is known that temporal variation of some compounds, such as carbon dioxide, can be quite large because the efficiency of the removal system degrades quickly when the reactant bed is almost consumed. The spatial variation of the contaminant concentration to our knowledge has not been estimated, but one can predicted that it can be significant due to nonuniformity of the air flow within habitat. This assumption is supported by information (Savina, unpublished data) on large spatial variations of the contaminant concentrations throughout the Mir Station under normal operating conditions.

2

NASA plans for extended human presence in Space Station and bases on the Moon and Mars in the 21st century (White and Lujan, 1989) raises serious questions about the adequacy of current air revitalization and monitoring system for long duration missions. Added to the risk of accidental contaminations, there is a concern (Logan, 1989) that Space Station would become an example of runaway tight (or sick) building syndrome (Godish, 1995; Mølhave, 1989), since there will not be a luxury of frequent returns to Earth for thorough cleaning, characteristic to the Space Shuttle missions.

It becomes apparent that a new generation air revitalization system should support such advanced functions as real-time air quality monitoring; health risk evaluation of the current situation and prediction of the future risks based on the extrapolation of the current trends; an early detection of a contamination event which in turn allows for preventive mitigation of the health hazard; and isolation of the contamination source, which would facilitate repair and clean-up. Essential components of such system are gas sensors, high performance on-board computer and algorithms and methods which provide required system functionality. The analysis of existing gas sensors technology (Kocache, 1994; Barry and Brackbenbury, 1991) indicate that the instrumentation needed for on-line multicomponent gas analysis is already available. In fact, a prototype combustion products analyzer has been flown as part of NASA program to develop capability to detect combustion products (James and Coleman, 1994). More advanced instrumentation can be expected to become available in the near future, including real-time particle detector suitable for space flights (NASA, 1989). At the same time, a computing power of available workstations suitable for on-board implementations is constantly increasing.

In this report we present our progress, results and findings in development of an integrated air quality modeling, monitoring, fault detection and isolation system (Figure 1). The focus of this year efforts was on development of distributed model of the air contaminants transport, the study of air quality monitoring techniques based on the model of transport process and on-line contaminant concentration measurements, and sensor placement. In the next chapter we discuss different approaches to the modeling of the spacecraft air contamination, and propose a three-dimensional

3

distributed parameter air contaminant dispersion model, applicable to both laminar and turbulent transport. We further proposed a two-dimensional approximation of a full scale transport model based on the spatial averaging of three-dimensional model over least important space coordinate. A computer implementation of the transport model is considered in the third chapter where we present a detailed development of two- and three-dimensional models illustrated by contaminant transport simulation results. In the fourth chapter we suggest the use of a well established Kalman filtering approach as a method for generating on-line contaminant concentration estimates based on both real time measurements and the model of contaminant transport process. We also show that high computational requirements of the traditional Kalman filter can render difficult its real-time implementation for high-dimensional transport model and propose a novel Implicit Kalman filtering algorithm which is shown to lead to an order of magnitude faster computer implementation in the case of air quality monitoring. Section five discusses sensor placement. In Conclusions we summarize our results, and outline the direction for next year's research.
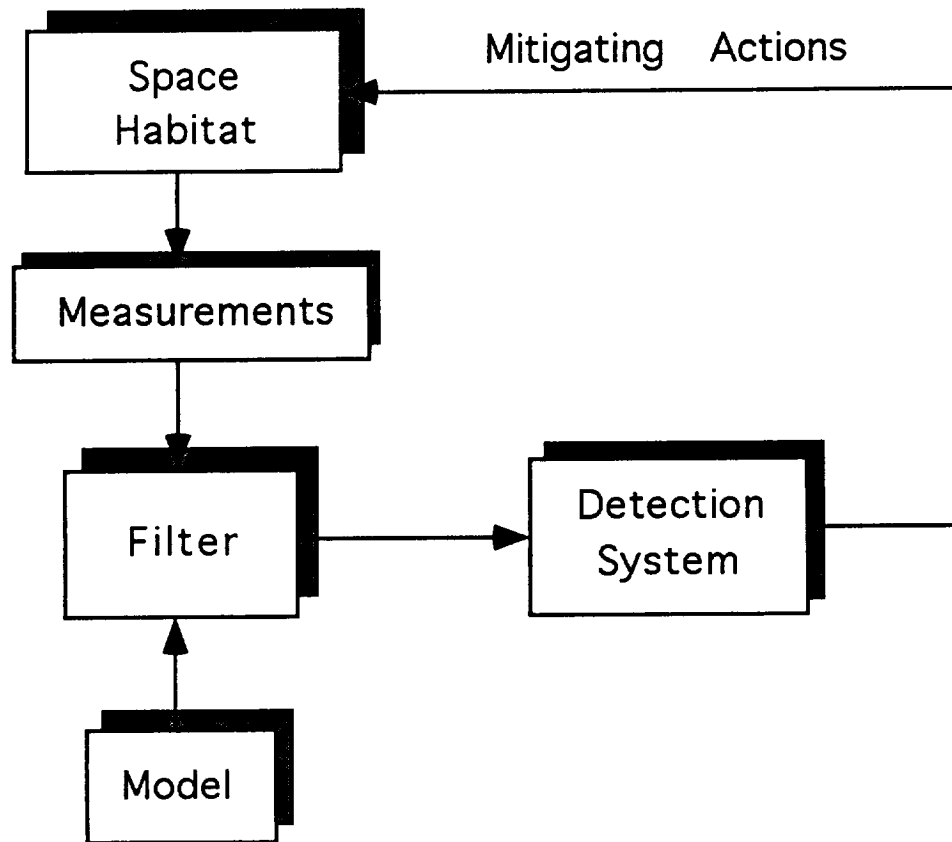
Figure 1.1: Integrated air quality monitoring system

Chapter 2

Dispersion Model of the Air Contaminants

2.1 Lumped and distributed models

Simulations of a spread, introduction and removal of airborne contaminants creates the basis for the solution of the entire complex of problems of monitoring and environmental control of a space habitat.

Generally, there are two different approaches to simulation. In the first one, each separate volume of a habitat, such as a cabin or a room, is represented as a well mixed tank with uniform distribution of all parameters. Mathematical models of this approach are a system of ordinary differential equations, resulting from the application of the macroscopic mass balances (National Academy of Sciences, 1981). The result of simulation is time change of volume-averaged concentration of different gaseous and airborne particulate contaminants, which depend on the rate of contaminants generation and removal. These models are relatively simple to develop and apply but are characterized by low resolution and accuracy.

An example of a computer model of this type is Trace Contaminant Control Simulation (TCCS) computer program (Perry, 1993), which was specifically designed to facilitate the development of a spacecraft contamination control hardware and prediction of its performance.

Another example is Computer Aided System Engineering and Analysis (CASE/A) modeling package for environmental control and life support system (ECLSS Integration Analysis, 1990), developed at McDonnell Douglas Space Systems Company. Although it also uses a well-stirred tank as an underlying representation of the habitat's volume, it belongs to a class of multi-tank models of indoor air quality (Ozkaynak et al., 1982; Ryan et al., 1988), and provides means for simulation of a number of connected tanks. This allows to model of different configurations with more than one interconnected volumes in habitat or to represent a single volume as a combination of well stirred-tanks thus increasing resolution and reliability of simulation results.

An alternative approach is to base the computer model on the fundamental distributed laws of physics. This results in the mathematical description of the process in the form of partial differential equations with appropriate initial and boundary conditions, and gives an exhaustive information on the distribution of contaminants throughout the spacecraft. However, its complexity and high computational requirements are obvious shortcomings.

In the analysis of the environmental risk of a space mission, the assessment of the effects of chronic inhalation of low concentration contaminants is at least as important as the analysis of extreme concentrations as a result of on-board accidents. Models of the spacecraft modules, based on the assumption of well mixed volumes cannot account for fluctuations in concentrations within a habitat. At the same time, effect of a higher than average concentration of contaminants and spatial distributing of the concentration can be significant, especially for long duration space missions. A distributed model is also needed to precisely identify unknown source of contamination. All these factors lead to a conclusion that the perspective of long-term and remote space missions requires the development of sophisticated models of the space habitat which can be run in real time, and serve as a basis for monitoring and decision making systems far more sophisticated than current detection and environmental control systems.

2.2 Three-dimensional model of the contaminant dispersion

According to Fick's law of molecular diffusion (Bird *et al.*, 1960), binary mass transport process with isotropic diffusion can be described by the following convection-diffusion equation:

$$\frac{\partial q}{\partial t} + (\nabla \cdot qU) = (\nabla \cdot D_M \nabla q) + F,$$
$$U = (u, v, w), \tag{2.1}$$

with an appropriate initial and boundary conditions, where q is the instantaneous contaminant concentration distribution within spatial domain Ω, D_M is the molecular diffusivity of contaminant in the air, U is the velocity distribution of the air flow, F is a source function describing generation and removal of the contaminant, and ∇ is the vector differential operator.

If the contaminant fraction in the air is low, equation (2.1) can also be used to describe a multicomponent transport. In this case, the spread of each contamination component is described by a model in form of equation (2.1). The transport models for different contaminants can be coupled through a generation term F, and a molecular diffusivity D_{Mi} in general depends on a particular type of the contaminant species.

If the density of the air is constant, equation (2.1) in rectangular coordinates yields

$$\frac{\partial q}{\partial t} + \frac{\partial uq}{\partial x} + \frac{\partial vq}{\partial y} + \frac{\partial wq}{\partial z} = (\nabla \cdot D_M \nabla q) + F, \tag{2.2}$$
$$x = (x, y, z) \in \Omega.$$

An appropriate boundary conditions for equation (2.2) correspond to impermeable wall, air duct, open hatch and completely or partially permeable wall (Table 1). For all practical purposes, source function F can be adequately described by the combination of pointwise contaminant sources and sinks:

$$F = \sum_{i=1}^{N_{so}} F_i^{so}(t)\delta(x - x_i^{so}) - \sum_{i=1}^{N_{si}} F_i^{si}(t)\delta(x - x_i^{si}), \tag{2.3}$$

where $(N_{so}, F_i^{so}, x_i^{so})$ and $(N_{si}, F_i^{si}, x_i^{si})$ are the number, capacity and location of a point source and sink, $x = (x, y, z)$, and δ is the Dirac delta function.

8

Equation (2.2) is directly applicable to the laminar transport of an airborne contaminant. Though results of Son and Barker, 1993 suggest that space station air flows will be mainly laminar, turbulent transport can play a significant role at least in some parts of the spacecraft habitat. Thus, it is important to modify (2.2) in order to accommodate the case of the turbulent transport.

For the case of turbulent flow, both the flow velocity $U = (u, v, w)$ and the concentration q must be treated as stochastic quantities. Following the framework of semi-empirical theory of turbulent diffusion (Bird *et al.*, 1960) we introduce the following notation:

$$U = \bar{U} + U' = (\bar{u}, \bar{v}, \bar{w}) + (u', v', w'),$$
$$q = \bar{q} + q', \tag{2.4}$$

where $\bar{U}$, $\bar{q}$ are time smoothed values and U', q' are instantaneous fluctuations. Since we are interested in a meaningful trend of contaminant concentration, rather than its stochastic fluctuations, we average the Fickian model (2.2) over a time interval ΔT long enough for the integral of instantaneous fluctuations to vanish. This yields

$$\frac{\partial \bar{q}}{\partial t} + \nabla \cdot (\overline{q'U'}) + \nabla \cdot (\bar{q}\bar{U}) = (\nabla \cdot D_M \nabla \bar{q}) + \bar{F}, \tag{2.5}$$

where an overbar denotes a time averaged value. According to semi-empirical theory of turbulent transport, the fluctuation moment $\overline{q'U'}$ can be approximated by the gradient relationship

$$\overline{q'U'} = -D_T \nabla \bar{q}, \tag{2.6}$$

where D_T is an empirical coefficient of eddy or turbulent diffusivity. Since

$$D_M \ll D_T, \tag{2.7}$$

molecular diffusion can be ignored, and resulting three-dimensional turbulent transport model becomes

$$\frac{\partial \bar{q}}{\partial t} + \nabla \cdot (\bar{q}\bar{U}) = (\nabla \cdot D_T \nabla \bar{q}) + \bar{F}. \tag{2.8}$$

It is important to note that the models for laminar (2.2) and turbulent (2.8) transport are of the same mathematical form. This allows us to use the same computer model for laminar, turbulent and mixed contaminant transport cases.

9

2.3 Two-dimensional approximation

In an attempt to develop a model which gives sufficient details about contaminant concentration profile and at the same time is simple enough to be run on-line, a two-dimensional approximation of the transport model (2.2) was previously suggested (Todd *et al.*, 1993; Todd *et al.*, 1994). The transport model can be simplified by averaging equation (2.2) over least important spatial coordinate. Assuming the averaging over z, define the height averaged concentration:

$$q_2 = \frac{1}{H} \int_0^H q \, dz, \tag{2.9}$$

where H is the habitat's height. Further assume that D_M does not change with z, and that (u, v) is a z-averaged air velocity vector. Integrating (2.2) with respect to z, and accounting for boundary condition $w(0) = w(H) = 0$ obtain

$$\frac{\partial q_2}{\partial t} + \frac{\partial u q_2}{\partial x} + \frac{\partial v q_2}{\partial y} = \frac{\partial}{\partial x} D_M \frac{\partial q_2}{\partial x} + \frac{\partial}{\partial y} D_M \frac{\partial q_2}{\partial y} + f, \tag{2.10}$$

where

$$f = \int_0^H F \, dz + D_M \left[\frac{\partial q}{\partial z} \bigg|_H - \frac{\partial q}{\partial z} \bigg|_0 \right]. \tag{2.11}$$

Similarly, a turbulent dispersion is approximated by the following two dimensional model:

$$\frac{\partial \bar{q}_2}{\partial t} + \frac{\partial \bar{u} \bar{q}_2}{\partial x} + \frac{\partial \bar{v} \bar{q}_2}{\partial y} = \frac{\partial}{\partial x} D_T \frac{\partial \bar{q}_2}{\partial x} + \frac{\partial}{\partial y} D_T \frac{\partial \bar{q}_2}{\partial y} + f, \tag{2.12}$$

where $\bar{q}_2$ is height averages and time smoothed contaminant concentration.

This approach provides the flexibility of using different two-dimensional approximations (resulted from the averaging along different spatial coordinates), depending on the current needs, or to simultaneously run more than one approximation to obtain more detailed information about the spread of the contaminant.

Chapter 3

Computer Implementation of the Transport Model

3.1 Two-dimensional model

The transport equation with an appropriate boundary conditions is used to develop a computer model of the transport process.

First, using finite difference or finite element method find an approximation of the spatial partial derivatives in the model equation. For two-dimensional model (equation (2.10) or (2.12)) let matrix A is a discrete analog of the spatial operator

$$\mathcal{L}_{\boldsymbol{x}}(\cdot) = \frac{\partial}{\partial x} D_M \frac{\partial}{\partial x} + \frac{\partial}{\partial y} D_M \frac{\partial}{\partial y} - \frac{\partial u}{\partial x} - \frac{\partial v}{\partial y},$$

obtained using finite differences. A semi-discrete analog of (2.10) in a vector form can now be written as

$$\frac{dq}{dt} = Aq + f, \tag{3.1}$$

where $q(t) = [q_1, \ldots, q_n]$ is a finite difference approximation of the concentration $q_2(x, y, t)$, $f(t)$ is an approximation of the source function $f(x, y, t)$ plus a contribution from the boundary conditions. If $\mathcal{L}_{\boldsymbol{x}}$ is approximated using five point stencil, the resulted operator A is n-by-n sparse matrix with five or less non-zero elements on each row. Dimension n of the system (3.1) depends on the spatial mesh used to approximate $\mathcal{L}_{\boldsymbol{x}}$.

Temporal discretization of equation (3.1) concludes the development of the discrete analog of the transport equation (2.10). In order to ensure numerical stability of the computer implementation, for a large range of time steps Δt it is advisable to use implicit approximation of the time derivative in (3.1). For instance, Crank-Nicolson approximation scheme results in the following unconditionally stable discrete model:

$$A_1 q_{m+1} = A_2 q_m + f_m,\qquad (3.2)$$

where m is a time index, $f_m = f(m\Delta t)$, and

$$A_1 = \left(\frac{I}{\Delta t} - \frac{1}{2}A\right)$$
$$A_2 = \left(\frac{I}{\Delta t} + \frac{1}{2}A\right),$$

where I is a unit matrix. Note that if coefficients of (2.10) are time dependent, matrices A_1 and A_2 will change with m.

The sparsity of the system (3.2) can be exploited to yield an efficient implementation of the computer model. The use of the indexed storage of matrices A_1 and A_2 leads to a significant reduction in the required computer memory, while utilization of the structure specific methods of matrix manipulation results in an efficient solution engine for linear system (3.2).

The details on development and implementation of two-dimensional transport model based on 5-point stencil approximation of spatial derivatives, Crank-Nicolson approximation in time domain, and spatial solution methods, which take advantage of a sparse structure of the discrete transport model are given in the next subsection

The finite elements method leads to the similar results. A spatial discretization in this case yields the following semi-discrete equation

$$M\frac{dq}{dt} = A_{fe}q + f_{fe},\qquad (3.3)$$

where M and A_{fe} are usually called mass and stiffness matrices. They are sparse, and depend on weight and element functions of the chosen finite element method, and on the ordering of the components of q. A source term f_{fe} is an approximation of $f(x, y, t)$ plus a contribution from the boundary conditions.

12

As before, a discrete analog is obtained as a result of the temporal approximation of the above semi-discrete equation. An implicit discretization yields a discrete model in the form of equation (3.2), where A_1 and A_2 depend on the specific scheme. One possible expression is

$$A_1 = \left(\frac{M}{\Delta t} - \frac{1}{2} A_{fe} \right)$$
$$A_2 = \left(\frac{M}{\Delta t} + \frac{1}{2} A_{fe} \right),$$

obtained using central difference approximation in time domain.

3.1.1 Computer implementation of two-dimensional transport model

The model equation (2.10) of the two-dimensional transport with appropriate boundary conditions is used to develop a computer model of the transport process. First, using finite difference approximations of the partial derivatives with respect to spatial coordinates we obtain a semi-discrete analog of the model equation. The diffusion operator is approximated as

$$\mathcal{D} \frac{\partial^2 q_2}{\partial x^2} \sim \mathcal{D}_{n,p} \frac{q_{n+1,p} - 2q_{n,p} + q_{n-1,p}}{\Delta x^2}, \tag{3.4}$$

$$\mathcal{D} \frac{\partial^2 q_2}{\partial y^2} \sim \mathcal{D}_{n,p} \frac{q_{n,p+1} - 2q_{n,p} + q_{n,p-1}}{\Delta y^2}, \tag{3.5}$$

where $q_{n,p} \sim q_2(t, n\Delta x, p\Delta y)$, Δx and Δy are discretization steps along coordinates x and y, $\mathcal{D}_{n,p}$ corresponds to $\mathcal{D} = \{D_M(n\Delta x, p\Delta y), D_T(n\Delta x, p\Delta y)\}$, and the subscript is used to specify a point on the spatial mesh $\{(n,p) \mid n = \overline{1,N}, p = \overline{1,P}\}$.

Since central difference approximation of the convective operator is known to cause non-physical oscillation of the numerical solution, the following upwind differencing scheme is used:

$$\frac{\partial u q_2}{\partial x} \sim u_{n,p} \frac{q_{n,p}^E - q_{n,p}^W}{\Delta x}, \tag{3.6}$$

where

$$q_{n,p}^E = \begin{cases} q_{n,p} & \text{if } u_{n,p} > 0, \\ q_{n-1,p} & \text{if } u_{n,p} < 0, \end{cases}$$

13

$$q_{n,p}^W = \begin{cases} q_{n-1,p} & \text{if } u_{n,p} > 0, \\ q_{n,p} & \text{if } u_{n,p} < 0. \end{cases}$$

Similarly,

$$\frac{\partial v q_2}{\partial y} \sim v_{n,p} \frac{q_{n,p}^S - q_{n,p}^N}{\Delta y}, \tag{3.7}$$

where

$$q_{n,p}^S = \begin{cases} q_{n,p} & \text{if } v_{n,p} > 0, \\ q_{n,p-1} & \text{if } v_{n,p} < 0, \end{cases}$$

$$q_{n,p}^N = \begin{cases} q_{n,p-1} & \text{if } v_{n,p} > 0, \\ q_{n,p} & \text{if } v_{n,p} < 0. \end{cases}$$

After spatial discretization the model equation take the following semi-discrete form:

$$\frac{dq_{n,p}}{dt} + u_{n,p} \frac{q_{n,p}^E - q_{n,p}^W}{\Delta x} + v_{n,p} \frac{q_{n,p}^S - q_{n,p}^N}{\Delta y}$$
$$= \mathcal{D}_{n,p} \left(\frac{q_{n+1,p} - 2q_{n,p} + q_{n-1,p}}{\Delta x^2} + \frac{q_{n,p+1} - 2q_{n,p} + q_{n,p-1}}{\Delta y^2} \right) + f_{n,p}^m. \tag{3.8}$$

The application of center difference approximation of the time derivative yields the following discrete analog of the two-dimensional transport model:

$$\frac{q_{n,p}^{m+1} - q_{n,p}^m}{\Delta t} = -\frac{1}{2} \left(u_{n,p} \frac{\left[q_{n,p}^E\right]^{m+1} - \left[q_{n,p}^W\right]^{m+1}}{\Delta x} + u_{n,p} \frac{\left[q_{n,p}^E\right]^m - \left[q_{n,p}^W\right]^m}{\Delta x} \right.$$
$$+ v_{n,p} \frac{\left[q_{n,p}^S\right]^{m+1} - \left[q_{n,p}^N\right]^{m+1}}{\Delta y} + v_{n,p} \frac{\left[q_{n,p}^S\right]^m - \left[q_{n,p}^N\right]^m}{\Delta y} \right)$$
$$- \mathcal{D}_{n,p} \left(\frac{q_{n+1,p}^{m+1} - 2q_{n,p}^{m+1} + q_{n-1,p}^{m+1}}{\Delta x^2} + \frac{q_{n,p+1}^{m+1} - 2q_{n,p}^{m+1} + q_{n,p-1}^{m+1}}{\Delta y^2} \right.$$
$$+ \frac{q_{n+1,p}^m - 2q_{n,p}^m + q_{n-1,p}^m}{\Delta x^2} + \frac{q_{n,p+1}^m - 2q_{n,p}^m + q_{n,p-1}^m}{\Delta y^2} \right) + f_{n,p}^m, \tag{3.9}$$

where Δt is the time discretization step, and the superscript $m = 0, 1, 2, \ldots$ is used to identify an instance $t = (m+1)\Delta t$ for which the solution of equation (3.9) is sought.

After collecting like terms in (3.9) obtain the following equation for a single spatial mesh point (n, p):

$$A q_{n-1,p}^{m+1} + B q_{n,p}^{m+1} + C q_{n+1,p}^{m+1} + D q_{n,p-1}^{m+1} + E q_{n,p+1}^m =$$

14

$$-Aq^m_{n-1,p} + Gq^m_{n,p} - Cq^m_{n+1,p} - Dq^m_{n,p-1} - Eq^m_{n,p+1} + f_{n,p}, \qquad (3.10)$$

where the coefficients are equal

$$
\begin{aligned}
A &= A_1 + A_2, \\
B &= B_1 + B_2, \\
C &= -\mathcal{D}_{n+1,p}\frac{\Delta y}{2\Delta x}, \\
D &= D_1 + D_2, \\
E &= -\mathcal{D}_{n,p+1}\frac{\Delta x}{2\Delta y}, \\
G &= G_1 + G_2, \qquad (3.11)
\end{aligned}
$$

where

$$
\begin{aligned}
A_1 &= -\frac{1}{2}\mathcal{D}_{n,p}\frac{\Delta y}{\Delta x}, \\
B_1 &= \frac{\Delta x \Delta y}{\Delta t} + \frac{\mathcal{D}_{n+1,p}\Delta y}{2\Delta x} + \frac{\mathcal{D}_{n,p+1}\Delta y}{2\Delta x} \\
&\quad + \mathcal{D}_{n,p}\left(\frac{\Delta y}{2\Delta x} + \frac{\Delta x}{2\Delta y}\right), \\
D_1 &= -\frac{\mathcal{D}_{n,p}\Delta x}{2\Delta y}, \\
G_1 &= \frac{\Delta x \Delta y}{\Delta t} - \frac{\mathcal{D}_{n+1,p}\Delta y}{2\Delta x} - \frac{\mathcal{D}_{n,p+1}\Delta y}{2\Delta x} \\
&\quad - \mathcal{D}_{n,p}\left(\frac{\Delta y}{2\Delta x} + \frac{\Delta x}{2\Delta y}\right), \qquad (3.12)
\end{aligned}
$$

and

$$
\begin{aligned}
A_2 &= \begin{cases} -\frac{u_{n,p}\Delta y}{2}, & u_{n,p} < 0, \\ \frac{u_{n,p}\Delta y}{2}, & u_{n,p} > 0, \end{cases} \\
D_2 &= \begin{cases} -\frac{v_{n,p}\Delta x}{2}, & v_{n,p} < 0, \\ \frac{v_{n,p}\Delta x}{2}, & v_{n,p} > 0, \end{cases} \\
B_2 &= B_3 + B_4 \\
B_3 &= \begin{cases} \frac{u_{n,p}\Delta y}{2}, & u_{n,p} < 0, \\ -\frac{u_{n,p}\Delta y}{2}, & u_{n,p} > 0, \end{cases} \\
B_4 &= \begin{cases} \frac{v_{n,p}\Delta x}{2}, & v_{n,p} < 0, \\ -\frac{v_{n,p}\Delta x}{2}, & v_{n,p} > 0, \end{cases} \\
G_2 &= G_3 + G_4,
\end{aligned}
$$

15

$$G_3 = \begin{cases} -\frac{u_{n,p}\Delta y}{2}, & u_{n,p} < 0, \\ \frac{u_{n,p}\Delta y}{2}, & u_{n,p} > 0, \end{cases}$$

$$G_4 = \begin{cases} -\frac{v_{n,p}\Delta x}{2}, & v_{n,p} < 0, \\ \frac{v_{n,p}\Delta x}{2}, & v_{n,p} > 0. \end{cases} \qquad (3.13)$$

The discrete transport model (3.10)-(3.13) is unconditionally stable and is free of non-physical oscillations. It has a second order accuracy in the time domain. Though, application of upwind differencing for convective operator results in only first order accuracy in space, the absence of numerical oscillation for all values of model parameters and discretization steps makes model (3.10)-(3.13) very attractive from the practical point of view.

3.1.2 Discrete model in the matrix form

The system of $N \times P$ equations of the form (3.10)-(3.13) describes a contaminant transport process within a spatial domain $0 \leq x \leq (N-1)\Delta x$, $0 \leq y \leq (P-1)\Delta y$. However, its exact appearance depends on how these equations are arranged into a single matrix equation. We have implemented a node numbering algorithm known as D4, or altering diagonals method (Aziz and Settari, 1979), which allow a particularly efficient direct solution of the model equation. According to this method, an equation describing each node (n, p) enters as i-th row of the overall matrix equation (3.2), where determination of i is summarized in Table 1.

The discrete transport model can now be written in the matrix form as

$$A_1 q_{m+1} = b, \qquad (3.14)$$

where vector $q_{m+1} = \{q_{n,p}^{m+1} \mid \overline{1,N}, \overline{1,P}\}$ approximates the contaminant concentration distribution on the time step $m+1$, A_1 is a sparse $NP \times NP$ matrix with at most five non-zero elements on each row, and

$$b = A_2 q_m + f_m, \qquad (3.15)$$

where f_m accounts for boundary conditions, and sources and sinks of contamination.

16

Even $(n + p)$	Odd $(n + p)$
For $(n + p) \leq N$ $i = \left(\frac{n+p}{2} - 1\right)^2 + p$	$(n + p) \leq (N + 1)$ $i = \frac{NP}{2} - \frac{(n-p+1)(n-p-3)}{4} - P$
For $N < n + p \leq P$ $i = \frac{(N-2)^2}{4}$ $-\frac{(N-1)^2 - N(n+p)-1}{2} - n$	For $N + 1 < n + p \leq P + 1$ $i = \frac{NP}{2} - \frac{N^2}{4}$ $+\frac{n+p}{2} N + 1 - n$
For $n + p > P$ $i = \frac{(N-2)^2}{4} + \frac{NP - N^2 - 2N}{2}$ $+\frac{(2N+P-n-p+4)(n+p-P)}{4}$ $-(n + 1)$	For $n + p > P + 1$ $i = NP - P + p$ $-\frac{(N+P-(n+p)+1)(N+P-(n+p)-1)}{4}$

Table 3.1: D4 Node Numbering Algorithm

3.1.3 Solution of the matrix equation (3.14)

The alternating diagonals node numbering method produces the discrete model (3.14) which can be partitioned as

$$\begin{bmatrix} A_{11} & A_{12} \\ A_{21} & A_{22} \end{bmatrix} \begin{bmatrix} q_{m+1}^1 \\ q_{m+1}^2 \end{bmatrix} = \begin{bmatrix} b_1 \\ b_2 \end{bmatrix}, \tag{3.16}$$

where A_{11}, A_{22} are diagonal matrices, and A_{12}, A_{21} are sparse matrices.

Special structure of equation (3.16) suggests a simple and efficient method of direct solution of matrix equation(3.14). First, by direct exclusion transform the lower half of the matrix equation (3.16) to obtain

$$\begin{bmatrix} A_{11} & A_{12} \\ 0 & \overline{A_{22}} \end{bmatrix} \begin{bmatrix} q_{m+1}^1 \\ q_{m+1}^2 \end{bmatrix} = \begin{bmatrix} b_1 \\ \overline{b_2} \end{bmatrix}. \tag{3.17}$$

A sparse matrix equation

$$\overline{A_{22}} q_{m+1}^2 = \overline{b_2} \tag{3.18}$$

of reduced order $\frac{NP}{2}$ s now independently solved for q_{m+1}^2 using Gaussian elimination. Given the solution of equation (3.18), q_{m+1}^1 is found as

$$q_{m+1}^1 = A_{11}^{-1} b_1 - A_{11}^{-1} A_{12} q_{m+1}^2, \tag{3.19}$$

17

where A_{11} is a diagonal matrix. Overall solution of (3.14) is now formed as

$$q_{m+1} = \begin{bmatrix} q_{m+1}^1 \\ q_{m+1}^2 \end{bmatrix}. \tag{3.20}$$

3.1.4 Simulation example.

For the cabin depicted in Figure 2 consider a two-dimensional height averaged approximation of the contaminant transport process. Assuming the laminar air flow, the parabolic input and output air velocities, and additional parameters presented in Table 2 we can calculate z-averaged air velocity distribution in the cabin as shown in Figure 3. Here arrows follow the streamlines of the air flow, and there length is proportional to the magnitude of the air velocity at a particular spatial point. The maximum air velocity is equal 1 m/s and occurs in the center of the air duct. Note that due to a large velocity gradients we have assumed $\mathcal{D} = 23$ cm^2/s, which is the eddy diffusivity of carbon dioxide in air.
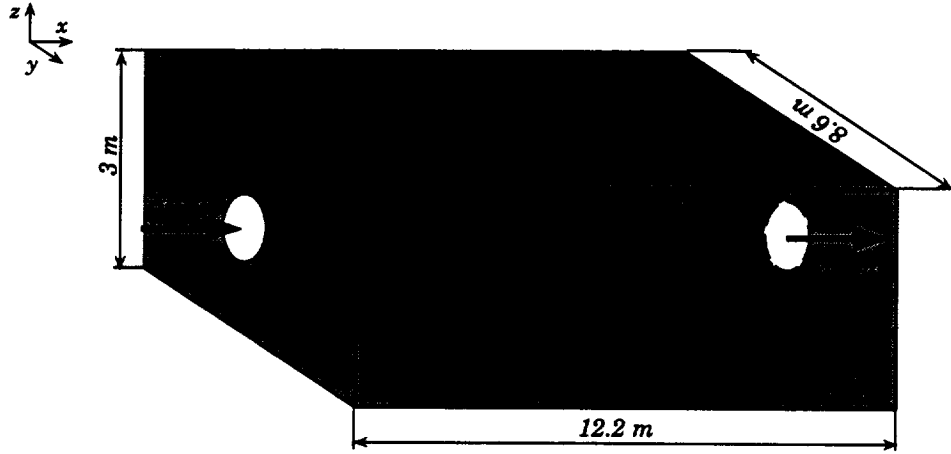

Figure 3.1: Simulated cabin geometry

Let us further assume that initially contaminant concentration in the cabin is zero, and that at the time $t = 0$ a contaminant is introduced into cabin with the inlet air stream at a known rate (Table 2).

Using this contamination scenario, we can calculate the evolution of the contaminant concentration distributions in the cabin. Results of the simulation 6 sec, 40 sec,
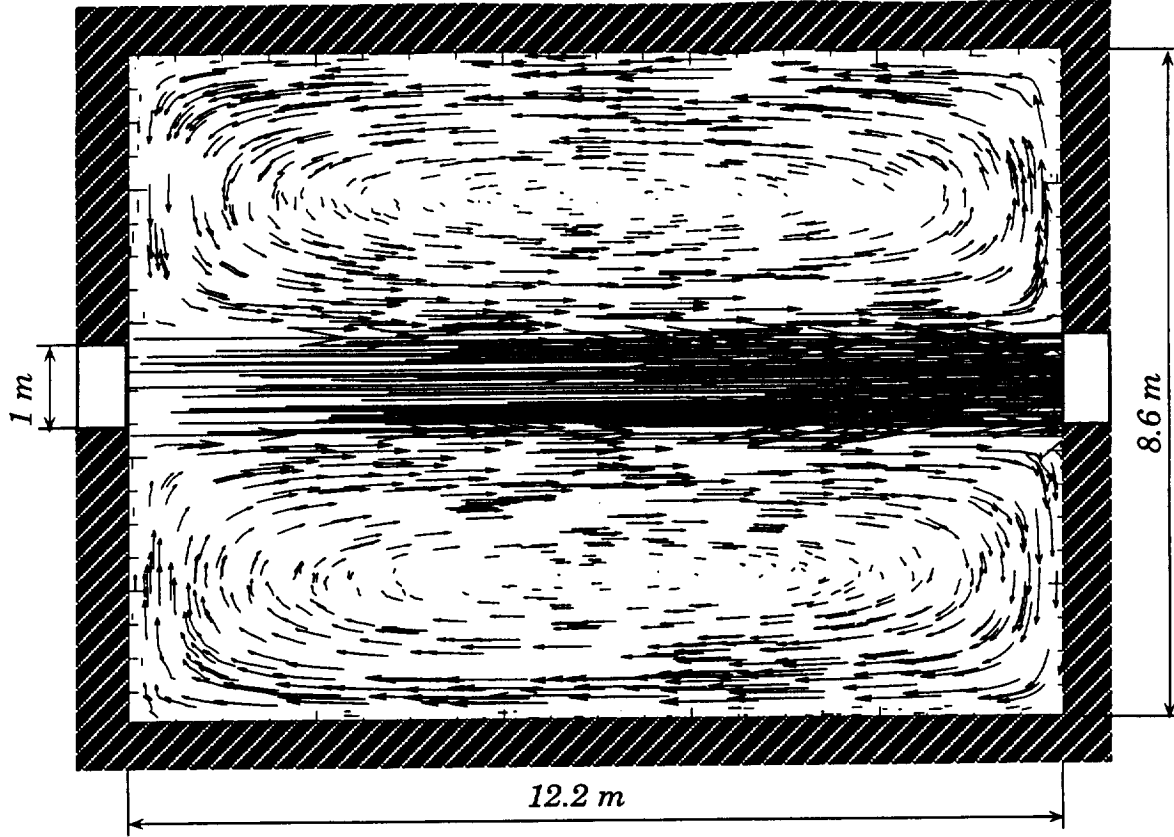
18

Figure 3.2: Height averaged air velocity distribution

2 *min*, 4 *min*, 6 *min* and 10 *min* 40 *sec* after the beginning of the emission are shown in Figure 4. At 10 *min* 40 *sec* contaminant distribution has already reached its steady state.

3.2 Three-dimensional model

Described two-dimensional design can be used to discretize the partial differential equation (2.1) or (2.8) to obtain a straight forward implementation of the three-dimensional transport model. However, the dimension n of the resulted system of the form (3.2) can be very large. At the same time, the structure of the sparse matrices A_1 and A_2 is more complicated in this case. Specifically, the width of the

19

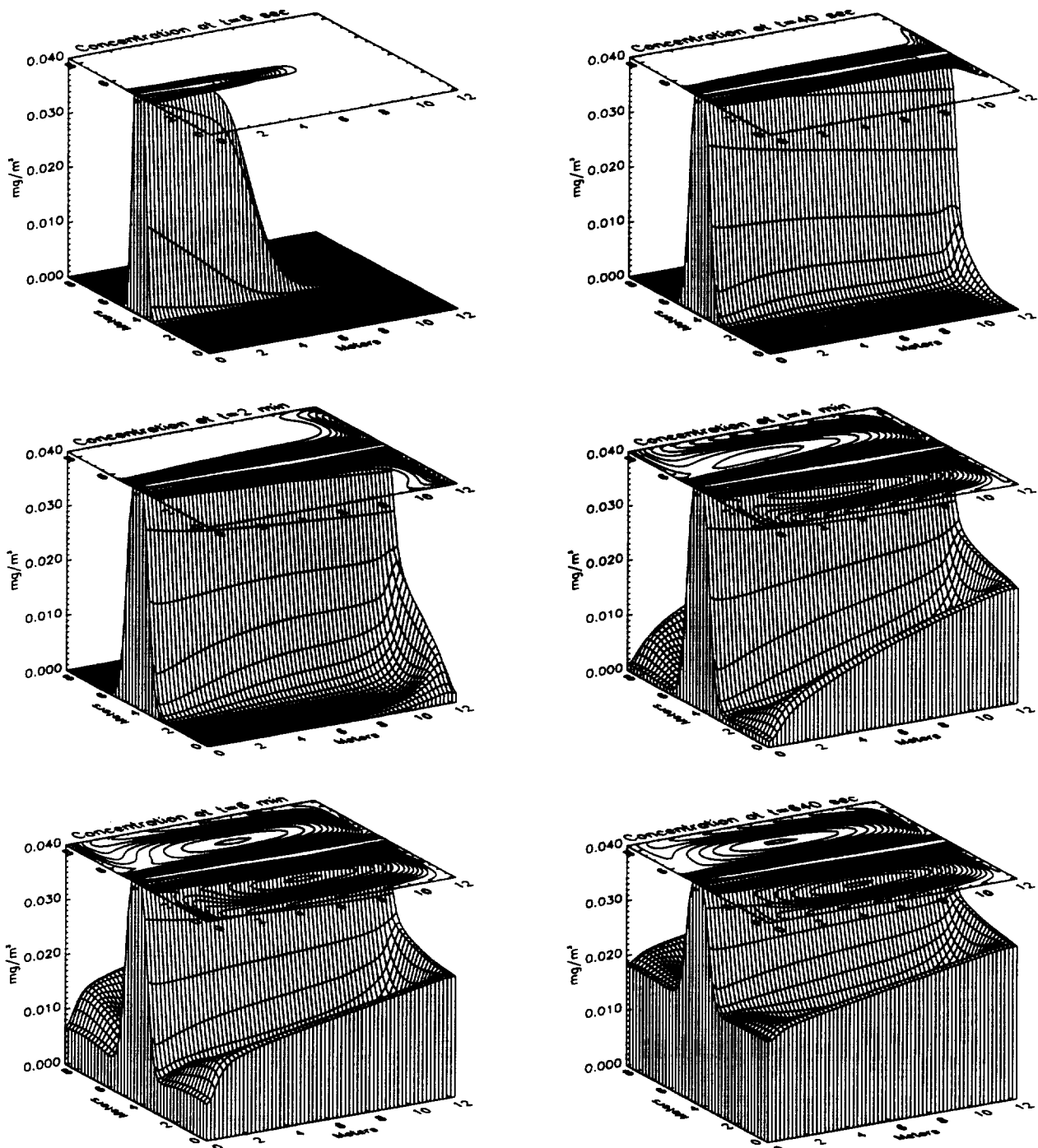Figure 3.3: Model predicted evolution of the contaminant dispersion

band in A_1 and A_2 can be substantial. Consequently, strait forward implementation three-dimensional transport model can be quite computer intensive.

A significant reduction in computational complexity can be achieved following the paradigm of the alternating-direction implicit (ADI) approach, which embodies the idea of operator or time splitting. Such splitting allows the reduction of the original problem into a series of simplified problems which must be solved consecutively on each time step. For example, the Douglas method leads to the following numerical implementation:

$$\left(-A_x - \frac{2}{\Delta t}\right) q^* = \left(A_x + 2A_y + 2A_z - \frac{2}{\Delta t}\right) q_m + 2f_m,$$
$$\left(-A_y - \frac{2}{\Delta t}\right) q^{**} = -A_y q_m - \frac{2}{\Delta t} q^*,$$
$$\left(-A_z - \frac{2}{\Delta t}\right) q_{m+1} = -A_z q_m - \frac{2}{\Delta t} q^{**}, \tag{3.21}$$

where q^* and q^{**} are intermediate variables, A_i is a finite difference approximation of the spatial operator $\mathcal{L}_i, : i = \{x, y, z\}$, where, for instance,

$$\mathcal{L}_x(\cdot) = \frac{\partial}{\partial x} D_M \frac{\partial}{\partial x} - \frac{\partial u}{\partial x}.$$

Thus, instead of solving one large and complex system (3.2) we need to solve three tridiagonal equation (3.21), which can be accomplished simply and efficiently.

Chapter 4

Air Quality Monitoring Using Kalman Filtering

A modeling of the introduction, dispersion, and removal of airborne contaminants in an enclosed environment is very important. It summarizes our knowledge about the transport process, and is especially valuable during the design stage, since it allows us to predict what happens under different scenarios of chronic or accidental contamination, analyze the influence of different factors on the spread of contaminants, simulate performance and limitations of air revitalization system, and use pre-recorded flight data to recreate and analyze real events occurring on-board of the spacecraft. At the same time, the model is merely a reflection of our current *a priori* knowledge about physics of the air contaminants transport process, geometry of the volume of interest, emission sources and removal devices. As a result, the quality of simulation depends solely on the assumptions employed in the development of the model, and completeness and accuracy of the input data.

In reality we almost never have all the required information and the adequateness of the model is often in question. Furthermore, a real system is subject to stochastic perturbation and information about some system parameters (such as eddy diffusivity) is inherently uncertain and incomplete. All this decreases the value of the results based solely on *a priori* knowledge and input data.

The most important information about air quality in a habitat is the concentration

distribution of the airborne contaminant, pre-selected for monitoring. The task of generating a real (or near real) time contaminant concentration estimates can only be accomplished using on-line concentration measurements. However, one should be aware of the limitations of the measurement data along. Practical considerations allow to deploy only a limited number of sensors. Each sensor produces spatially localized (i.e. pointwise) information, which is corrupted by noise, and requires filtering. The measurements from different sensors may not be in complete agreement requiring data fusion and reconciliation. And finally, localized (pointwise) measurement data must be extrapolated over the entire habitated volume to obtain complete contaminant concentration distribution.

All these serves as a motivation for developing the air quality monitoring system based on both on-line measurements, and the verified model of the transport process. The integration of the measurement data and the model can be achieved within the framework of the well established Kalman filtering method. According to Kalman filtering paradigm the uncertainties of the model and measurements are represented by the additive stochastic white Gaussian perturbation. First, lets consider the modification of the transport model. For the transport model in rectangular coordinates (2.2), the modified stochastic model of the process takes the following form:

$$\frac{\partial q}{\partial t} + \frac{\partial uq}{\partial x} + \frac{\partial vq}{\partial y} + \frac{\partial wq}{\partial z} = (\nabla \cdot D_M \nabla q) + F + c(\boldsymbol{x}, t) w(\boldsymbol{x}, t), \qquad (4.1)$$

$$q(\boldsymbol{x}, 0) = q^0(\boldsymbol{x}),$$

$$\mathrm{E}[q^0(\boldsymbol{x})] = 0, \quad \mathrm{E}[q^0(\boldsymbol{x}_1) q^0(\boldsymbol{x}_2)] = p_0(\boldsymbol{x}_1, \boldsymbol{x}_2),$$

$$\boldsymbol{x}, \boldsymbol{x}_1, \boldsymbol{x}_2 \in \Omega,$$

with an appropriate boundary conditions, where $c(\boldsymbol{x}, t)$ is a deterministic function of noise intensity, $w(\boldsymbol{x}, t)$ is Gaussian white (in time) process with zero mean, and

$$\mathrm{E}[w(\boldsymbol{x}_1, t) w(\boldsymbol{x}_2, \tau)] = Q(\boldsymbol{x}_1, \boldsymbol{x}_2, t) \delta(t - \tau),$$

where $\mathrm{E}[\cdot]$ and $\delta(\cdot)$ are the expectation operator and the Dirac delta function, Q and p_0 are nonnegative function, symmetric in the sense that $Q(\boldsymbol{x}_1, \boldsymbol{x}_2, t) = Q(\boldsymbol{x}_2, \boldsymbol{x}_1, t)$, and $p_0(\boldsymbol{x}_1, \boldsymbol{x}_2) = p_0(\boldsymbol{x}_2, \boldsymbol{x}_1)$.

The process model (4.1) must be further supplemented with the model of the measurement system, reflecting our knowledge on how the actually available sensors' output relates to the state of the process q. In a general form, measurement system can be represented as

$$z(x, t) = h(q, t) + v(x, t), \quad x \in \Omega, \tag{4.2}$$

where $z(x, t)$ is the output of the measurement system, $h(q, t)$ is a spatial measurement operator (usually linear), and $v(x, t)$ is Gaussian white process independent of $w(x, t)$ with zero mean and nonnegative symmetric covariance function R:

$$E[v(x_1, t)v(x_2, \tau)] = R(x_1, x_2, t)\delta(t - \tau), \quad x_1, x_2 \in \Omega.$$

Currently available sensor usually can provide only pointwise readings. A general model of the measurement system (4.2) in this case take form

$$z(x_j, t) = h(q(x_j, t), t) + v(x_j, t), \quad j = 1, \ldots, l,$$

where x_j is a sensor's location, and l is a total number of sensors.

The level of the model and the measurements uncertainties is determined by the covariance functions Q and R. The choice of the measurement noise covariance matrix R is made based on the careful study of the sensing instrumentation in the controlled conditions. The covariance of the model noise is chosen at the model validation stage and depends on how well the model reflects the real process. After initial determination of Q and R they are often viewed as a design parameters, and can be further adjusted to obtain desired estimates.

A theory of the Kalman filtering for distributed parameter systems (Tzafestas, 1982; Ray and Lainiotis, 1978) can be readily applied to the system (4.1)-(4.2). However, resulted distributed Kalman filter equation, and an associated nonlinear distributed Ricatti equation must eventually be transformed into a discrete form to enable a numerical solution of the filtering problem.

Alternatively, the Kalman filtering can be applied to a discrete analog of the distributed parameter system (4.1)-(4.2) to begin with. Though not as theoretically

sound, this approach presents some practical advantages since it is less mathematically involved, and is more general in the sense that it leads to an implementation of the Kalman filter which is less dependent on the changes in the process model.

The discretization of the stochastic model (4.1) concludes in a discrete analog in the form of either a single implicit equation (3.2), or a system of implicit equations, such as the system (3.21).

First, consider the case of implicit equation (3.2), appropriately modified and supplemented with the discrete analog of the measurement equation (4.2):

$$
\begin{aligned}
A_1 q_{m+1} &= A_2 q_m + f_m + C(m) w_m, && (4.3) \\
q_0 &= q^0, \\
z_{m+1} &= H(m+1) q_{m+1} + v_{m+1} && (4.4)
\end{aligned}
$$

where $C(m)$ and $H(m+1)q_{m+1}$ are discrete approximations of $c(x, m\Delta t)$ and $h(q, (m+1)\Delta t)$, and z_{m+1} is a measurement vector corresponding to $z(x, t)$; w_m and v_{m+1} are uncorrelated zero mean white Gaussian sequences such that

$$
\begin{aligned}
E[w_j w_m^T] &= Q(m)\delta(j - m), \\
E[v_{j+1} v_{m+1}^T] &= R(m+1)\delta(j - m),
\end{aligned}
$$

where $Q(m)$ and $R(m+1)$ approximate functions $Q(x_1, x_2, m\Delta t)$ and $R(x_1, x_2, (m+1)\Delta t)$, and $\delta(j - m) = 1$ if $j = m$ and zero otherwise.

The traditional Kalman filtering require that the model be given in the explicit form. If matrix A_1 in non-singular for all m, the implicit model (4.3) can be rewritten in an equivalent explicit form, and the traditional Kalman filter can be applied to generate the optimal estimates of q_{m+1}. However, there is a strong motivation to avoid matrix inversion step in a filtering algorithm. If for some m matrix A_1 is ill-conditioned, its inverse is calculated with significant error, unless some special measures are built into the filtering algorithm. This would usually involve on-line calculation of the condition number of A_1 and application of iterative improvement in order to calculate the explicit model equation with acceptable accuracy, or the use of a singular value decomposition as a first step in calculating matrix inversion.

Furthermore, the system matrix $A_1^{-1}A_2$ of the equivalent explicit representation must be treated as general (full) matrix, since inversion destroys matrix sparsity. Therefore, application of the traditional Kalman filtering can leads to significant computational errors should the matrix A_1 be ill-conditioned, and results in an inefficient algorithm due to the need to manipulate full (non-sparse) matrices.

We have previously proposed an implicit Kalman filtering method (Skliar and Ramirez, 1995a, b), which does not require matrix inversion, and when applied to a sparse implicit system is an order of magnitude faster than the traditional Kalman filter, making it a superb method for on-line estimation of the contaminant concentration.

According to the implicit Kalman filter method, the optimal concentration estimate $\hat{q}_{m+1|m+1}$ is given by the following implicit Kalman filter equation:

$$A_1\hat{q}_{m+1|m+1} = \hat{y}_{m+1|m} + L_y(m+1)\left[z_{m+1} - H_1(m+1)\hat{y}_{m+1|m}\right] \tag{4.5}$$

for $m = 0, 1, ...$, where

$$\hat{y}_{m+1|m} = A_2\hat{q}_{m|m} + f_m \tag{4.6}$$

with $\hat{q}_{0|0} = \hat{q}^0$, and the modified the measurement matrix $H_1(m+1)$ is determined by the linear equation

$$H_1A_1 = H. \tag{4.7}$$

The implicit Kalman filter gain $L_y(m+1)$ is equal

$$L_y(m+1) = P^y_{m+1|m+1}H_1^T(m+1)R^{-1}(m+1)$$
$$= P^y_{m+1|m}H_1^T(m+1)\left[H_1(m+1)P^y_{m+1|m}H_1^T(m+1) + R(m+1)\right]^{-1} \tag{4.8}$$

where the predicted estimation error covariance matrix $P^y_{m+1|m}$ of an auxiliary variable $y(m+1) = A_1q_{m+1}$ is found as a result of the time propagation of the estimation error covariance $P^q_{m|m}$ of the concentration q_m according to equation

$$P^y_{m+1|m} = A_2P^q_{m|m}A_2^T + C(m)Q(m)C^T(m). \tag{4.9}$$

The estimation error covariance matrix $P^y_{m+1|m+1}$ satisfies the covariance measurement update equation

$$P^y_{m+1|m+1} = P^y_{m+1|m} - P^y_{m+1|m}H_1^T(m+1)$$

26

$$\times \left[H_1(m+1)P^y_{m+1|m}H_1^T(m+1) + R^{-1}(m+1) \right]^{-1} H_1(m+1)P^y_{m+1|m} \quad (4.10)$$

or equivalently

$$P^y_{m+1|m+1} = \left[I - L_y(m+1)H_1(m+1) \right] P^y_{m+1|m}. \quad (4.11)$$

The error covariance matrix $P^q_{m+1|m+1}$ of the concentration estimate $\hat{q}_{m+1|m+1}$ is related to the covariance matrix $P^y_{m+1|m+1}$ by the following linear matrix equation:

$$P^y_{m+1|m+1} = A_1 P^q_{m+1|m+1} A_1^T. \quad (4.12)$$

The implicit Kalman filter generates the minimal variance estimations of q_{m+1}, and is theoretically equivalent to the traditional Kalman filtering, provided the inverse of matrix A_1 exist for all k. However, it provides a basis for a new implementation algorithm for the implicit system (4.3) which does not require matrix inversion. This makes it a superior approach when matrix A_1 is ill-conditioned or sparse.

We now formulate an algorithm to determine the optimal estimate of the state q_{m+1} of the system (4.3), (4.4) using the implicit Kalman filter. Given z_{m+1}, $\hat{q}_{m|m}$ and $L_y(m+1)$,

1. Compute $\hat{y}_{m+1|m}$ by propagating $\hat{q}_{m|m}$ according to equation (4.6).

2. Solve the linear matrix equation (4.7) for the modified measurement matrix $H_1(m+1)$.

3. Solve the linear equation

$$A_1 \hat{q}_{m+1|m+1} = \hat{y}_{m+1|m} + L_y(k+1) \left[z_{m+1} - H_1(m+1)\hat{y}_{m+1|m} \right] \quad (4.13)$$

for the optimal estimate $\hat{q}_{m+1|m+1}$.

If matrices A_1 and H are time invariant, matrix H_1 needs to be calculated only once. The Kalman gain $L_y(m+1)$ can be calculated in the following ways. Given $P^q_{m|m}$,

1. Compute $P^y_{m+1|m}$ by propagating $P^q_{m|m}$ according to equation (4.9).

2. Compute the implicit Kalman filter gain using equation (4.8).

3. Calculate $P^y_{m+1|m+1}$ according to equation (4.11).

Note that in order to initiate the gain calculation algorithm on the next time step, we need to find $P^q_{k+1|k+1}$ from the linear equation (4.12), using direct or iterative methods of solution.

Turning attention to a discrete analog of the stochastic transport model (4.1)-(4.2) in the form of the system of implicit equations we immediately observe that after appropriate modifications system (3.21) can be written a single implicit equation

$$A_1 Q_{m+1} = A_2 Q_m + \begin{bmatrix} 2f_m \\ 0 \\ 0 \end{bmatrix} + \begin{bmatrix} 2C(m) \\ 0 \\ 0 \end{bmatrix} w_m, \qquad (4.14)$$

where

$$Q_m = \begin{bmatrix} q^*_m \\ q^{**}_m \\ q_m \end{bmatrix},$$

$$A_1 = \{A^{ij}_1\} = \begin{bmatrix} \left(-A_x - \frac{2}{\Delta t}\right) & 0 & 0 \\ \frac{2}{\Delta t} & \left(-A_y - \frac{2}{\Delta t}\right) & 0 \\ 0 & \frac{2}{\Delta t} & \left(-A_z - \frac{2}{\Delta t}\right) \end{bmatrix},$$

$$A_2 = \{A^{ij}_2\} = \begin{bmatrix} 0 & 0 & \left(A_x + 2A_y + 2A_z - \frac{2}{\Delta t}\right) \\ 0 & 0 & -A_y \\ 0 & 0 & -A_z \end{bmatrix},$$

and

$$z_{m+1} = [0 \ \ 0 \ \ H(m+1)] \, Q_{m+1} + v_{m+1}. \qquad (4.15)$$

The system (4.14)-(4.15) is in the same form as (4.3)-(4.4), and the implicit Kalman filter is directly applicable. Resulted algorithm can be further simplified if a special structure of (4.14) is taken into account. After obvious transformations, the estimation of the contaminant concentration is determined from the sequential solution of the following tridiagonal equations:

$$\left(-A_x - \frac{2}{\Delta t}\right) q^* = \left(A_x + 2A_y + 2A_z - \frac{2}{\Delta t}\right) \hat{q}_{m|m} + 2f_m + L_1[z - H_1 \hat{y}_{m+1|m}],$$

$$\left(-A_y - \frac{2}{\Delta t}\right) q^{**} = -A_z \hat{q}_{m|m} - \frac{2}{\Delta t} q^{**} + L_2[z - H_1 \hat{y}_{m+1|m}],$$

$$\left(-A_z - \frac{2}{\Delta t}\right) \hat{q}_{m+1|m+1} = -A_z \hat{q}_{m|m} - \frac{2}{\Delta t} q^{**} + L_3[z - H_1 \hat{y}_{m+1|m}], \qquad (4.16)$$

where the predicted estimation of the auxiliary variable $y = A_1 Q$ is equal

$$\hat{y}_{m+1|m} = \begin{bmatrix} A_2^{13} \\ A_2^{23} \\ A_2^{33} \end{bmatrix} \hat{q}_{m|m} + \begin{bmatrix} 2f_m \\ 0 \\ 0 \end{bmatrix}. \qquad (4.17)$$

The modified measurement matrix $H_1 = \{H_{1j}\}$ is found from the following linear equation:

$$[H_{11} \ H_{12} \ H_{13}]A_1 = [0 \ 0 \ H],$$

solution of which reduces to the solution of the following three linear tridiagonal equations :

$$\begin{cases} H_{13} A_1^{33} = H, \\ H_{12} A_1^{22} = -H_{13} A_1^{32}, \\ H_{11} A_1^{11} = -H_{12} A_1^{21}. \end{cases} \qquad (4.18)$$

The implicit Kalman gain $L_{m+1} = [L_1^T \ L_2^T \ L_3^T]^T$ is equal

$$L_{m+1} = P_{m+1|m}^y H_1^T \left[H_1 P_{m+1|m}^y H_1^T + R(m+1) \right]^{-1}, \qquad (4.19)$$

where

$$P_{m+1|m}^y = \begin{bmatrix} A_2^{13} P_{m|m}^q A_2^{13T} + 4CQC^T & A_2^{13} P_{m|m}^q A_2^{23T} & A_2^{13} P_{m|m}^q A_2^{33T} \\ A_2^{23} P_{m|m}^q A_2^{13T} & A_2^{23} P_{m|m}^q A_2^{23T} & A_2^{23} P_{m|m}^q A_2^{33T} \\ A_2^{33} P_{m|m}^q A_2^{13T} & A_2^{33} P_{m|m}^q A_2^{23T} & A_2^{33} P_{m|m}^q A_2^{33T} \end{bmatrix}. \qquad (4.20)$$

As before,

$$P_{m+1|m+1}^y = [I - L_{m+1} H_1] P_{m+1|m}^y, \qquad (4.21)$$

and

$$P_{m+1|m+1}^y = A_1 P_{m+1|m+1}^Q A_1^T,$$

where $P_{m+1|m+1}^Q = \left\{ \left[P_{m+1|m+1}^Q \right]^{ij} \right\}$, $i,j = \{1,2,3\}$ is the covariance matrix of the estimation error of Q.

Taking the advantage of the block-matrix structure of A_1, the solution of the last equation is reduced to a sequential solution of the following six tridiagonal equations:

$$
\begin{cases}
A_1^{11}\left[P^Q_{m+1|m+1}\right]^{11}A_1^{11T} = \left[P^y_{m+1|m+1}\right]^{11}, \\[2mm]
A_1^{11}\left[P^Q_{m+1|m+1}\right]^{12}A_1^{22T} = \left[P^y_{m+1|m+1}\right]^{12} - A_1^{11}\left[P^Q_{m+1|m+1}\right]^{11}A_1^{21T}, \\[2mm]
A_1^{11}\left[P^Q_{m+1|m+1}\right]^{13}A_1^{33T} = \left[P^y_{m+1|m+1}\right]^{13} - A_1^{11}\left[P^Q_{m+1|m+1}\right]^{12}A_1^{32T}, \\[2mm]
A_1^{22}\left[P^Q_{m+1|m+1}\right]^{22}A_1^{22T} = \left[P^y_{m+1|m+1}\right]^{22} - A_1^{21}\left[P^Q_{m+1|m+1}\right]^{11}A_1^{21T} \\[2mm]
\qquad\qquad\qquad - A_1^{21}\left[P^Q_{m+1|m+1}\right]^{12}A_1^{22T} - \left[A_1^{21}\left[P^Q_{m+1|m+1}\right]^{12}A_1^{22T}\right]^T, \\[2mm]
A_1^{22}\left[P^Q_{m+1|m+1}\right]^{23}A_1^{33T} = \left[P^y_{m+1|m+1}\right]^{23} - A_1^{21}\left[P^Q_{m+1|m+1}\right]^{12}A_1^{32T} \\[2mm]
\qquad\qquad\qquad - A_1^{22}\left[P^Q_{m+1|m+1}\right]^{22}A_1^{32T} - A_1^{21}\left[P^Q_{m+1|m+1}\right]^{13}A_1^{33T}, \\[2mm]
A_1^{33}\left[P^Q_{m+1|m+1}\right]^{33}A_1^{33T} = \left[P^y_{m+1|m+1}\right]^{33} - A_1^{32}\left[P^Q_{m+1|m+1}\right]^{22}A_1^{32T} \\[2mm]
\qquad\qquad\qquad - A_1^{32}\left[P^Q_{m+1|m+1}\right]^{23}A_1^{33T} - \left[A_1^{32}\left[P^Q_{m+1|m+1}\right]^{23}A_1^{33T}\right]^T,
\end{cases}
$$

$$(4.22)$$

where $\left[P^Q_{m+1|m+1}\right]^{33} = P^q_{m+1|m+1}$.

We are now in the position to formulate an algorithm for estimation of the contaminant concentration q_{m+1} based on the measurement data (4.15) and the transport model (4.14). Given z_{m+1}, $\hat{q}_{m|m}$ and L_{m+1},

1. Compute $\hat{y}_{m+1|m}$ by propagating $\hat{q}_{m|m}$ according to equation (4.17).

2. Successively solve three tridiagonal matrix equations (4.18) for the modified measurement matrix H_1.

3. Successively solve three tridiagonal equations (4.16) for the optimal estimation $\hat{q}_{m+1|m+1}$.

The calculation of the gain L_{m+1} of the implicit Kalman filter follows the following algorithm:

1. Calculate $P^y_{m+1|m}$ according to equation (4.20).

2. Calculate the implicit Kalman filter gain using equation (4.19).

3. Calculate $P^y_{m+1|m+1}$ according to equation (4.21).

4. To initiate the gain calculation algorithm on the next time step, sequentially solve six tridiagonal matrix equations (4.22) for the error covariance matrix $P^q_{m+1|m+1}$.

Despite the complex appearance, presented implicit filtering algorithm is very effective for the large dimension $\dim q_m = n$, and is convenient for computer implementation. If the number of sensors $l \ll n$, then the computer implementation of each the implicit filtering algorithm requires on the order of n^2 floating point operations, while the traditional explicit filter will require $O(n^3)$. Additionally, all linear systems that need to be solves in the course of implicit filtering have the same simple tridiagonal form, and a single solution engine can be used to implement the proposed algorithm.

Finally, it is well known, that for real-time applications of the Kalman filtering it is advisable to use a square root implementation algorithm, which has a superior numerical stability. The details on the square root implementation of the implicit Kalman filter can be found in Skliar and Ramirez (1996).

Chapter 5

Sensor Placement for Contamination Detection

A discrete time and discrete location algorithm for state estimation and the placement of monitoring devices (sensors) in a distributed parameter contaminant simulation is described, implemented, tested in a simple contaminant scenario, and compared to Extended Kalman filtering results. The state estimation portion of the algorithm is a suboptimal variation of Extended Kalman Filtering. The sensor placement portion of the algorithm is based on the minimization of the trace of the prediction error covariance matrix. It utilizes variables from the suboptimal state estimation portion of the algorithm with a yes/no type of switching algorithm to optimize the placement and number of the sensors in a set of pre-specified locations.

5.1   Introduction to sensor placement

Determination of the optimal number, type, and placement of sensors in a habitat is important to both ground-based applications and future space applications. "Tight" terrestrial buildings do not allow the free exchange of building air with the outside air, resulting in a buildup of stale air and potentially harmful toxicants in the building. Monitoring devices in the building can alert the building supervisors to high levels of toxicants and indicate when the building must be ventilated, but these monitoring devices must be placed in locations which can yield appropriate and useful information. It is presently not feasible from either a cost or a logistics stand-point to place sensors everywhere in a building that designers or operations personnel may deem them desirable.

Space habitats can be considered "tight" buildings, but with the added constraint that they cannot be ventilated with relatively clean outside air, the time-honored mitigation measure for ground-based buildings. It is therefore important to detect potentially harmful buildups of toxicants earlier than in terrestrial buildings, and alternative mitigation steps must then be taken. The increased detection requirements in space habitats increase the complexity of the monitoring system; but once again, sensors cannot be placed everywhere in the habitat. In addition to the obvious cost of the sensors, the cost of the information processing equipment, the limits on the physical placement of sensors in the habitat, and the cost to transport the mass associated with the sensors (from the Earth to the space habitat) motivates the space habitat designer to minimize the number of sensors used in the monitoring system.

5.2   Korbicz sensor location algorithm basics

A prospective algorithm for sensor location has been developed. It is based upon the algorithm, developed by Prof. Józef Korbicz (1986, 1988, 1991) and, uses Kalman Filter system observation techniques to place a limited number of sensors at selected locations in a two-dimensional area. This analysis technique can be expanded to three-dimensions but with more intensive computations. (The contaminant concentration in a compartment volume has been traditionally averaged over the height of the compartment so that a two-dimensional analysis can be performed on a three-dimensional space.) The algorithm minimizes the contaminant concentration prediction error at selected points in the analysis area, based on the sensor readings of a specified sensor configuration, and thereby increases the estimation accuracy of the contaminant concentration. The algorithm is able to determine a near-optimal placement of a specified number of sensors in specified locations, given the dispersion of a contaminant as described by a distributed parameter model, and given the desired concentration monitoring accuracy. The suboptimal algorithm of Korbicz is reportedly more computationally efficient than previous algorithms due to its approximation of the prediction error covariance matrix.

A distributed parameter model is a mathematical model of a system that is described by a set of partial-differential equations. This is contrasted to a lumped parameter model, which is a mathematical model of a system that is generally described by a set of ordinary differential equations. The distributed parameter model attempts to describe the system in terms of the contaminant dispersion and removal processes in both time and spatial location, hence the dependent variables are functions of more than one independent variable, and partial differential equations are required. The lumped parameter model attempts to describe the system in coarser terms of the bulk flows and movements of contaminants in the system as a function only of time, discounting the distances between and within the "well-mixed" lumped nodes; hence, the dependent variables are only functions of time, and only ordinary differential equations are required.

While the Kalman Filtering algorithm can be used on both lumped parameter systems and distributed parameter systems, the filtering algorithm described below is developed around and will use a distributed parameter system. But in order to simulate the spread of contaminants in the model of the space habitat at discrete times, the system model has been basically reduced to small lumped nodes. The concentrations at these nodes are functions of both time and the distances to the adjacent nodes.

The equations have been coded for the suboptimal filtering algorithm (J. Korbicz, 1986), and for the sensor placement algorithm described in subsequent papers (J. Korbicz et al., 1988; J. Korbicz, 1991). The suboptimal filtering algorithm differs from a standard Kalman filter in that it approximates the prediction error covariance matrix through a discrete, time-stepping algorithm. The suboptimal filter equations generate state estimates, prediction and filtering errors, and the prediction error covariance estimator from given measurements.

The sensor location algorithm determines the optimal placement of N' spatially-fixed sensors to be distributed over N potential locations ($N \geq N'$, maximum of one sensor per location) in a 2-dimensional spatial configuration to monitor the distribution of one chemical species concentration. The methodology of the measurement location optimization is to minimize a cost functional, based on the trace of the prediction error covariance matrix. The sensor location algorithm uses data generated by the suboptimal filtering algorithm to

generate adjoint variables, which are the dynamic constraints for the minimization of a cost functional.

The sensor location algorithm uses a yes/no decision algorithm for the optimal placement of N' sensors in N locations. A switching function, based on the Hamiltonian of the optimal sensor problem, determines whether a sensor is or is not placed at a specified location. With the switching function having yes or no as the decision options, this measurement problem can be considered as a "bang-bang" control problem.

Inputs to the Korbicz Sensor Location Algorithm include the possible sensor locations within the habitat, the habitat system's distributed parameter equations (contaminant generation and spread), the level of noise that a sensor generates, the level of "process noise" from the habitat, and the required monitoring accuracy. Outputs from the Korbicz Sensor Location Algorithm are the minimum number of sensors required to meet a specified filtering accuracy (one aspect of a minimum cost sensor configuration), and the specific placement of those sensors to achieve that accuracy.

The system process noise from the habitat is the amount of contaminant concentration variability acknowledged in the dynamics (generation and spread) of the contaminant in the habitat due to airflow variability, disturbances, etc.

Example

A simple two-dimensional example will be used to demonstrate how an optimal sensor location algorithm works. Assume that the habitat atmosphere layout is rectangular as pictured in Figure 1a. The atmospheric system is gridded to allow observation of contaminant concentration over spatial locations within its whole area at n = 30 locations (grid intersections). A contaminant generation and dispersion model is applied to the habitat. The possible sensor locations are the five circles (N = 5). These are all of the permissible locations of sensors, denoted by the location vector $\underline{x}^*$ = ((1,3),(2,1),(3,5),(4,3),(5,2)). The locations may have been chosen for a variety of engineering and other reasons.
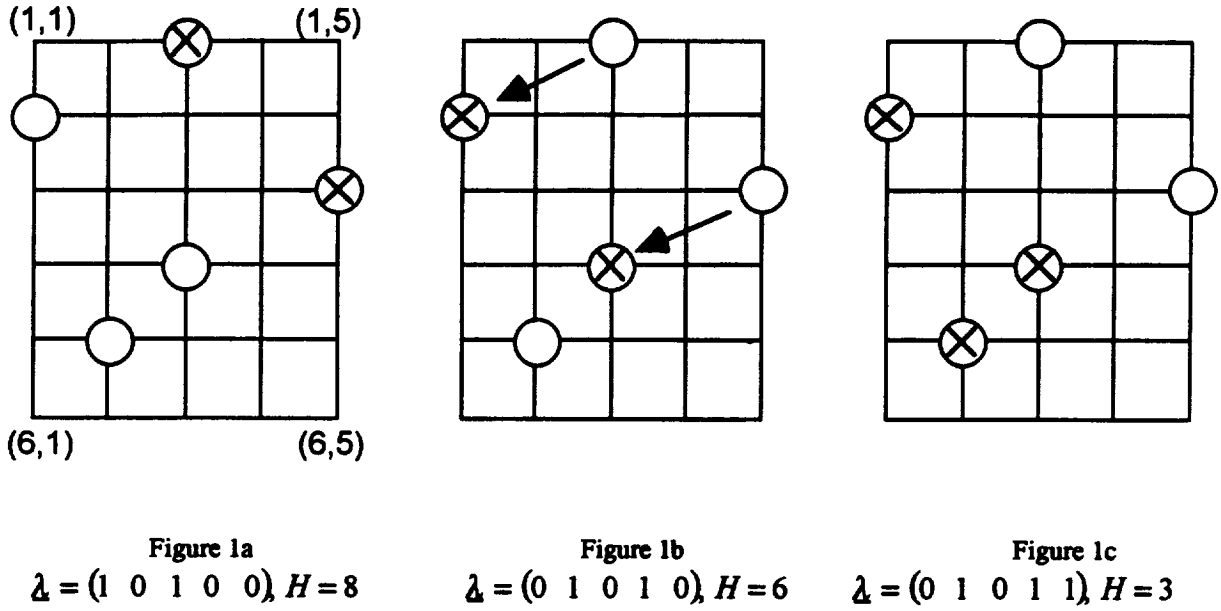
Figure 1. Movement of Sensors Using Sensor Location Algorithm

The algorithm continues by guessing at the number and placement of sensors in a sensor configuration. The habitat model has a certain amount of confidence, reflected in the system process noise, and each sensor has a defined noise level (noise generated by the sensor). Our initial guess is to place two sensors, $N' = 2$, at the locations marked with X's in Figure 1a, corresponding to the vector $\underline{\lambda} = (1\ 0\ 1\ 0\ 0)$. The placed sensors are used to monitor the habitat in a simulation, and an estimate of the concentration levels at selected points in the habitat (states) are calculated. The adjoint variables are calculated and the accuracy with which the sensors monitor the contaminant concentration can be judged by comparing the prediction error to a pre-determined error threshold.

Other monitoring parameters can be used as auxiliary measures, such as comparing the estimated contaminant concentration levels against the known levels of the contaminant concentration at the points, calculating the percentage of maximum peak concentration predicted versus the known percentage of maximum peak concentration, or calculating the Hamiltonian of the system. For our initial placement of sensors, the scalar Hamiltonian, H, is calculated to be 8. Maximizing or minimizing the Hamiltonian of a system corresponds to minimizing or maximizing a cost functional (such as the prediction error), according to the discrete maximum principle of Pontryagin. This will be described in more detail later; for

36

now let us assume that we want to minimize the prediction error, and therefore minimize the Hamiltonian.

Using a cost function based on the state prediction errors, the sensors are then shifted (via yes/no choices) to other locations, $\underline{\lambda} = (0\ 1\ 0\ 1\ 0)$, to provide a possible increase in accuracy until shifting of the sensors no longer helps, as shown in Figure 1b. The resulting error of this "best" configuration is then tested. The resulting value of the Hamiltonian in our example has been reduced to $H = 6$. If the desired accuracy (comparing predicted or estimated concentration states against the model's actual concentrations) is attained using some computed configuration with that number of sensors, then the number of sensors is decreased and the algorithm rerun until the desired accuracy is unattainable. If the desired accuracy is unattainable with using only two sensors (our desired accuracy threshold corresponds to $H < 4$), then three sensors can be tried, $\underline{\lambda} = (0\ 1\ 0\ 1\ 1)$, as shown in Figure 1c. This testing and retesting is continued until one of the previous successful configurations is revisited. The resulting set of sensors is a feasible suboptimal configuration of the number and locations of the sensors as determined by the Korbicz algorithm, and the algorithm stops. Our example found the Hamiltonian to be $H = 3$ for our third configuration, which reflected a minimized error in the state prediction estimate.

5.3 Simplified space habitat model

A simple, distributed-parameter, contaminant transport system model based on a model in one of Korbicz's early papersJ. Korbicz, 1986 was used as a baseline model. The simplified model consists of a tubular space, with eleven equal-distant "grid" points at which the contaminant concentration levels are desired to be known or estimated. This is illustrated in Figure 2. The points are $\Delta x = 0.1$ distance units apart. This is a very simple model, but can be considered to be similar to the interior of a cylindrical habitat, inside of which a contaminant is dispersing. In this model, the primary transport mechanism considered is diffusion, with a small factor of removal of the contaminant. This small contaminant removal might be considered as deposition of the contaminant on the walls of the habitat.
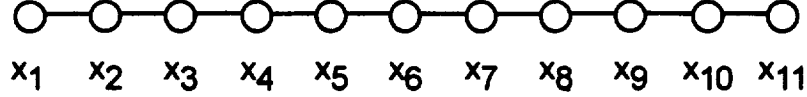
Figure 2. Simplified Discrete Habitat Model

The transport of the contaminant within this non-linear system is described by the continuous model,

$$\frac{\partial y(\underline{x}, t)}{\partial t} = D \times \frac{\partial^2 y(\underline{x}, t)}{\partial \underline{x}^2} - b \times \frac{y(\underline{x}, t)}{1 + |y(\underline{x}, t)|} + u(\underline{x}, t) + w(\underline{x}, t),$$

$$\text{(change)} = \text{(diffusion)} - \text{(deposition)} + \text{(control)} + \text{(noise)} \tag{5.1}$$

where $y(\underline{x}, t)$ is the contaminant concentration vector at locations $\underline{x}$ at time t. The discrete-time model of the continuous system of Eqn. (1) can be approximated by,

$$y(\underline{x}, k+1) = N_x(y, \underline{x}, k) + A(\underline{x}, k) \times u(\underline{x}, k) + B(\underline{x}, k) \times w(\underline{x}, k), \tag{5.2}$$

where,

$$N_x(y, \underline{x}, k) = y(\underline{x}, k) + \Delta t \times \left\{ D \times \frac{\partial^2 y(\underline{x}, k)}{\partial \underline{x}^2} - b \times \frac{y(\underline{x}, k)}{1 + |y(\underline{x}, k)|} \right\}, \tag{5.3}$$

$$A(\underline{x}, k) = \Delta t \times I, \tag{5.4}$$

$$B(\underline{x}, k) = I. \tag{5.5}$$

The system was initialized at concentration values of $y(\underline{x}, k = 0) = 0.4$. The diffusion coefficient was set to $D = 1$ and the removal coefficient was set to $b = 0.05$, essentially removing the removal term from affecting the contaminant concentration (but still accounting for it mathematically). The discrete, white. gaussian system process noise, $w(\underline{x}, k)$, was specified to have a mean of zero,

$$E[w(\underline{x}, k)] = 0, \tag{5.6}$$

38

and a (discrete) variance of $\sigma_w^2 = 0.0016$, resulting in a covariance matrix of,

$$Q(\underline{x},\underline{x}',k) = \begin{bmatrix} 0.0016 & & 0 \\ & \ddots & \\ 0 & & 0.0016 \end{bmatrix}.$$

(5.7)

The values of Q reflect the fact that the standard deviation of the model uncertainty of each state is $\sigma_w = 0.04$, or 4% of the steady-state values of the states, which are at concentrations of $y(\underline{x},k = \infty) = \sim 1$ at steady-state. $w(\underline{x},k)$ is also independent over time.

A step input contaminant flow to the system was input at the $\underline{x}_{11}$ location at time $t = 0.01$ sec., and the contaminant concentration was held at unity for the duration of the simulation, for,

$$y(\underline{x}_{11}, t \geq 0.01) = 1.$$

(5.8)

Other than the step input, no "control" inputs were used ($u(\underline{x},k) = 0$). The equations used to calculate the linearized response are (A is a tri-diagonal system matrix),

$$\dot{\underline{y}}(\underline{x}, t) = A \times y,$$

(5.9)

where,

$$A = \begin{bmatrix} \left(\frac{-D}{\Delta x^2} - \frac{b}{2}\right) & \frac{D}{\Delta x^2} & & & 0 \\ \frac{D}{\Delta x^2} & \left(\frac{-2D}{\Delta x^2} - \frac{b}{2}\right) & \frac{D}{\Delta x^2} & & \\ & \frac{D}{\Delta x^2} & \ddots & \ddots & \\ & & \ddots & \left(\frac{-2D}{\Delta x^2} - \frac{b}{2}\right) & \frac{D}{\Delta x^2} \\ 0 & & & \frac{D}{\Delta x^2} & \left(\frac{-D}{\Delta x^2} - \frac{b}{2}\right) \end{bmatrix}.$$

(5.10)

The removal term, $b \times \dfrac{y(\underline{x}, k)}{1 + |y(\underline{x}, k)|}$, from Eqn. (3) was linearized into $b \times \dfrac{b(\underline{x}, k)}{2}$ by letting $|y(\underline{x}, k)| = 1$, the idealized steady-state value of all y. The last row of A was set to zeros only for the simulation of the step input in the contamination scenario so as to not diminish the step input level; the non-zero system model values were used for the input to the Kalman Filter.

Because this simple system is so well connected, it is observable using only one sensor at any location. This was tested by examining the rank of the observability matrix (G.J. Smith, 1995). This system brings out an important aspect of testing for observability. It was necessary to normalize the system matrix of Eqn. (10) to accurately test for observability; otherwise, the rank of the observability matrix was calculated to be less than full because of the cutoff tolerance of the rank testing subroutine. Also, even though this system is observable with using only one sensor, that does not mean that all of the system states can be accurately estimated, as we shall see later in this paper.

5.4   Extended Kalman filter algorithm

The Kalman Filtering technique is a good method to obtain state information about states which are not directly measured, and is used as a baseline algorithm for the example. The Extended Kalman Filter is used for nonlinear systems, as compared to a basic Kalman Filter which is used for linear systems. Using the methods outlined in (W.F. Ramirez, 1994), an Extended Kalman Filter was written, using a least squares estimator, to estimate the contaminant concentration state at each of the eleven locations. Candidate sensor locations are at $\underline{x}_1$, $\underline{x}_6$, $\underline{x}_{11}$. The sensors were specified to have a noise variance of 0.0025 (which yields a standard deviation noise level in the sensor measurements of 0.05, in the units of the concentration being measured).

Using the Extended Kalman Filter algorithm, steady-state values of the prediction error covariance matrix and the Kalman gain matrix were calculated, using groupings of two sensors or three sensors, distributed one sensor per candidate sensor location maximum. Using those steady-state estimation matrices in the filtering equations, estimates of the states at each location were then calculated. The estimates of the states were compared to

the "actual states", and the absolute values of those differences were summed and averaged over the duration of the simulation. This average estimate error magnitude can be considered one measure of the accuracy of the Kalman filter. Note that the trace of the prediction error covariance matrix, calculated for each configuration, is not a good representation of effectiveness of the estimation when one sensor configuration is compared against another configuration. The base equations for the Extended Kalman Filter are presented below, adapted from 1994). The system and measurement models are given by,

$$y(\underline{x}, k+1) = F(y, k) + B(\underline{x}, k) \times w(\underline{x}, k), \tag{5.11}$$

$$z(k) = N_H(y, k) + v(k), \tag{5.12}$$

where $y(\underline{x}, k+1)$ is the updated system state vector, $z(k)$ is the measurement vector, $w(\underline{x}, k)$ is the white gaussian system process noise vector, $B(k)$ is a multiplicative factor matrix, and $v(k)$ is the white gaussian sensor noise vector. The non-linear system is modeled by the vector function $F(y, k)$. The non-linear measurements are modeled by the vector function $N_H(y, k)$. The system model variables are assumed to be defined at the locations $\underline{x}$, and the measurement model variables are assumed to be defined at the locations $\underline{x}^*$. The Extended Kalman Filter equations are,

$$\bar{y}(\underline{x}, k) = F(\hat{y}, \underline{x}, k-1) + B(k-1) \times w(\underline{x}, k-1), \tag{5.13}$$

$$P(k) = M(k) - M(k)\left(\frac{\partial N_H(k)}{\partial y(k)}\right)^T\left[\left(\frac{\partial N_H(k)}{\partial y(k)}\right)M(k)\left(\frac{\partial N_H(k)}{\partial y(k)}\right)^T + R(k)\right]^{-1}\left(\frac{\partial N_H(k)}{\partial y(k)}\right)M(k),$$

$$\tag{5.14}$$

$$K(k) = P(k) \times \left(\frac{\partial N_H(k)}{\partial y(k)}\right)^T \times R^{-1}(k), \tag{5.15}$$

$$M(k+1) = \left(\frac{\partial F(y,k)}{\partial y(k)}\right) \times P(k) \times \left(\frac{\partial F(y,k)}{\partial y(k)}\right)^T + B(k) \times Q(k) \times B^T(k), \tag{5.16}$$

$$\hat{y}(x,k) = \bar{y}(x,k) + K(k) \times \left(z(k) - N_H(\bar{y},k)\right). \tag{5.17}$$

The vector $\bar{y}(\underline{x},k)$ is the system state estimates before measurement (based upon the previous estimate), and $\hat{y}(\underline{x},k)$ is the system state estimate vector after measurement. $K(k)$ is the Kalman Filter gain matrix. $P(k)$ is the state error covariance matrix after measurement, while $M(k)$ is the state error covariance matrix before measurement.

5.5   Extended Kalman filter results

The accuracy of the Extended Kalman Filter was first tested using sensors at each of the three candidate locations, which yielded a time-averaged state error of 0.01343 (in the units of the concentration). The state error is the average difference between the actual contaminant concentration values, obtained from Eqn. (11), and the estimated state concentrations, obtained from Eqn. (17), including the concentrations at all eleven state locations in the average. For this sensor configuration, the trace of the prediction error covariance matrix, tr(M), was 0.03256 (in the units of the concentration squared). Table 1 shows the results using the Extended Kalman FIlter.

Table 1. Results of Extended Kalman Filter

Sensor Placement $\underline{\lambda} = \begin{bmatrix} \lambda_{(\underline{1})} & \lambda_{(\underline{1})} & \lambda_{(\underline{1\underline{1}})} \end{bmatrix}$	Average State Error
[1 1 1]	0.01343
[1 1 0]	0.04205
[1 0 1]	0.01247
[0 1 1]	0.01199

Next, only two sensors were used to supply the measurement information required by the Kalman Filter to estimate the states. The worst estimates were obtained when sensors were placed at locations x_1 & x_6, which yielded a time-average state error of 0.04205. Sensors were then placed at locations x_1 & x_{11}, and the resulting time-average state error was 0.01247, a significant improvement. The best estimates were obtained when sensors were placed at locations x_6 & x_{11}, which yielded a time-average state error of 0.01199. The plotted actual model concentrations and the estimated concentrations for this sensor configuration are shown in Figure 3. This sensor configuration was even better than the simulation run using three sensors. This is probably because the weightings being used place too much emphasis on the sensor measurements in our simulation. Heavier reliance on sensor measurements are good during disturbances, but not good during steady-state conditions.

From these results, it is seen that it is important to have a sensor at the location of the contaminant source (highest concentration). With one of the two sensors placed at x_{11}, placing the other sensor at location x_6 yielded only slightly better results than placing the other sensor at location x_1.

5.6   Korbicz suboptimal filtering algorithm

The algorithm for the suboptimal placement of the sensors is in two parts, the suboptimal filtering algorithm equations and the suboptimal sensor placement algorithm equations.

5.6.1 Objective Function

The purpose of the suboptimal filtering equations is to calculate the estimated value of the states, denoted by $\hat{y}$, such that the estimate is very close to the actual value of the states, y. This is primarily accomplished by calculating a filter gain matrix, denoted by K, which adjusts the computation of the estimated states. The filter gain matrix is based on the minimization of the discrete linear Kalman filter performance objective function, J,

$$J = \tfrac{1}{2}\left\{(y - \hat{y})^T \times M^{-1} \times (y - \hat{y})\right\} + \tfrac{1}{2}\left\{(z - Hy) \times R^{-1} \times (z - Hy)^T\right\}, \quad (5.18)$$

43

actual non-linear and estimated (– –) states (x1, x6, x11)

N = 2 –> [6 11] , Extended Kalman Filter
Qi = 0.0016 , Ri = 0.0025
trace P = 0.05489 , ave. error ≈ 0.01199
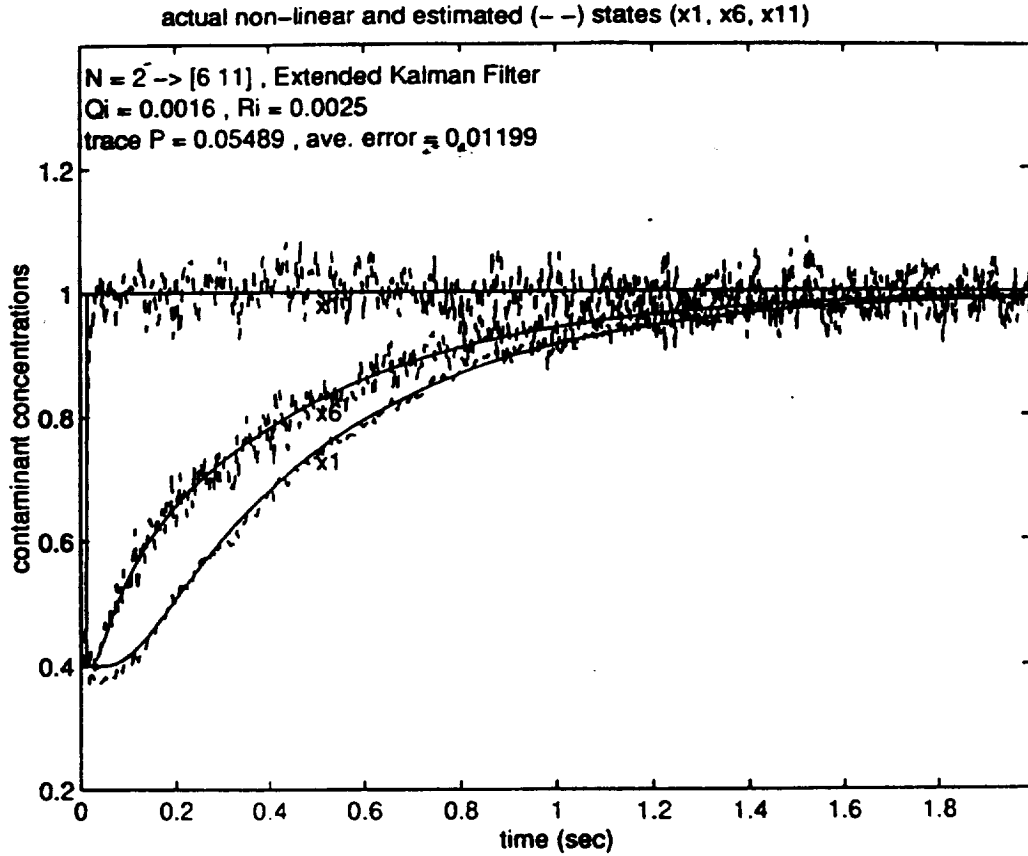
Figure 3. Extended Kalman Filter Estimate of States, Sensors at x_6 & x_{11}, Response to a Step Input at Location x_{11}

where H is the measurement matrix, R is the covariance matrix of the sensor noise, z is the actual measurements, and M is the prediction error covariance matrix (before measurement). The first term of this objective function minimizes the deviation between the new state and the state estimate before the new measurements are taken, while the second term minimizes deviations between the actual measurements and their computed values (W.F. Ramirez, 1994).

From the minimization of Eqn. (18), we obtain a value for M, which leads directly to the computation of the filter gain K (that equation is stated later). The product of the filter gain matrix K and the innovation error (difference between the actual measurement and the predicted measurements) is then added to the system model predicted states to yield new values for the estimated states. In short, the filter gain matrix adjusts the system model's predicted states based on the measurement errors to yield better state estimates, which are

44

then fed into the system model again. This algorithm, extracted from (J. Korbicz, 1986; J. Korbicz et al., 1988; J. Korbicz, 1991) is described in more detail below.

5.6.2 Algorithm Equations for a General System

A system can be described by n states within a connected open spatial domain Ω, where the states are at spatial locations, $\underline{x}$, within the spatial coordinate vector, $\underline{x}$, in the spatial domain of Ω (as before). For simplicity, we shall assume that the number of states equals the number of spatial locations, and therefore consider only one contaminant.

The states of the system, y (an n-dimensional state vector), are discretized at iteration step times k. The time iteration runs from 0 through K. The states are calculated using a system model function, N_X (state update differential operator vector), and incorporating system process noise. The system process noise weighting matrix function is denoted by B, and w is the white gaussian system process noise of the individual states (the noise inherent in the dynamics of the system). The state of the system at time $k+1$, $y(\underline{x},k+1)$ is equal to the update differential operator given information from time k, $N_X(y,\underline{x},k)$, plus system noise, Bw.

$$y(\underline{x},k+1) = N_X(y,\underline{x},k) + B(\underline{x},k) \times w(\underline{x},k), \quad k = 0,...,K \tag{5.19}$$

The covariance of the system process noise is given by Q, and is assumed to be uncorrelated across time.

Out of the n states, N states (discrete measurement points in the coordinate spaces) are measured at times k, and the measurements are denoted by z, the observation vector at the selected points. The selected physical locations are denoted by $\underline{x}^*$, which is a subset of $\underline{x}$. The measurements z incorporate sensor noise denoted by v.. For linear systems, the measurement matrix H transforms the states y into measurements z. For non-linear systems, this transformation is denoted by $N_H(y,k)$, a vector function at the measurement points.

$$z(\underline{x},k) = \left[z(\underline{x}_1^*,k) z(\underline{x}_2^*,k)...,z(\underline{x}_N^*,k) \right]^T = N_H(y,k) + v(k) \approx H \times y(\underline{x},k) + v(k). \tag{5.20}$$

The state vector at the measurement points is denoted by y^*,

$$y^*(x,k) = \left[y(x_1^*,k) y(x_2^*,k) ..., y(x_N^*,k) \right]^T .$$

(5.21)

The white gaussian measurement noise v (the noise generated by the sensors) at the instrumented locations is derived from R, the specified covariance of the measurement noise, and is uncorrelated between sensors.

The state estimates, $\hat{y}$, are calculated from the state propagation function, N_x, and adjusted by the product of the filter gain, K, and the measurement prediction error, v (also called the innovation error).

$$\hat{y}(x,k+1|k+1) = N_x(\hat{y},x,k|k) + K(x,k+1) \times v(k+1) .$$

(5.22)

The innovation error, v, is a vector which calculates the difference between the actual state measurements, z, and the predicted measurements, $N_H(\hat{y}, k+1|k)$,

$$v(k+1) = z(k+1) - N_H(\hat{y}, k+1|k) .$$

(5.23)

The initial state estimate at the points in the system is set to $\hat{y}_0$,

$$\hat{y}(x,k|k)|_{k=0} = \hat{y}_0(x) .$$

(5.24)

The system filter gain (weighting) matrix, K, is derived from the product of the prediction error covariance matrix, M, the calculated trends of the state measurements as predicted by the model, $(N_H)_{\hat{y}}$ (a Jacobian matrix), and the inverse of the Γ matrix.

$$K(x,k+1) = M(\hat{y},x,k+1|k) \times (N_H)_{\hat{y}} \times \Gamma^{-1}(k+1|k),$$

(5.25)

where,

$$\left(N_H\right)_{\hat{y}} = \frac{\partial N_H}{\partial y^T}\bigg|_{y=\hat{y}} = \begin{vmatrix} \dfrac{\partial N_H\left(y,x_1^*,k\right)}{\partial \hat{y}(x_1,k)} & \dfrac{\partial N_H\left(y,x_1^*,k\right)}{\partial \hat{y}(x_2,k)} & \cdots & \dfrac{\partial N_H\left(y,x_1^*,k\right)}{\partial \hat{y}(x_n,k)} \\ \dfrac{\partial N_H\left(y,x_2^*,k\right)}{\partial \hat{y}(x_1,k)} & \ddots & & \vdots \\ \vdots & & & \\ \dfrac{\partial N_H\left(y,x_N^*,k\right)}{\partial \hat{y}(x_1,k)} & & \cdots & \dfrac{\partial N_H\left(y,x_N^*,k\right)}{\partial \hat{y}(x_n,k)} \end{vmatrix},$$

(5.26)

The Γ matrix includes the covariance of the measurement noise, R, and the prediction error covariance matrix, M, adjusted by the predicted state measurement gradients, $\left(N_H\right)_{\hat{y}}$.

$$\Gamma(k+1|k) = R(k+1) + \left(N_H\right)_{\hat{y}}^T \times M(k+1|k) \times \left(N_H\right)_{\hat{y}}.$$

(5.27)

If the measurement matrix H in Eqn. (20), has only one non-zero numerical value in each row, and zeros elsewhere, then each measurement, z, corresponds to an individual state. Therefore, the jacobian matrix $\left(N_H\right)_{\hat{y}}$ from Eqns. (25) & (27), and expanded in Eqn. (26), will have the same values as H.

The state prediction error, $\tilde{y}(\underline{x}, k+1|k) \cong y(\underline{x}, k+1) - \hat{y}(\underline{x}, k+1|k)$, is calculated using the state estimate error, $\tilde{y}(\underline{x}, k|k) \cong y(\underline{x}, k) - \hat{y}(\underline{x}, k|k)$, updating it by the calculated trends of each state, $\left(N_x\right)_{\hat{y}}$ (a Jacobian matrix), and including a noise component.

$$\tilde{y}(\underline{x}, k+1|k) = \left(N_x\right)_{\hat{y}} \times \tilde{y}(\underline{x}, k|k) + B(\underline{x}, k) \times w(\underline{x}, k),$$

(5.28)

where,

$$\left(N_x\right)_{\hat{y}} = \frac{\partial N_x}{\partial y^T}\bigg|_{y=\hat{y}} = \begin{vmatrix} \dfrac{\partial N_x(y_1)}{\partial \hat{y}_1} & \dfrac{\partial N_x(y_1)}{\partial \hat{y}_2} & \cdots & \dfrac{\partial N_x(y_1)}{\partial \hat{y}_N} \\ \dfrac{\partial N_x(y_2)}{\partial \hat{y}_1} & \ddots & & \vdots \\ \vdots & & & \\ \dfrac{\partial N_x(y_N)}{\partial \hat{y}_1} & & \cdots & \dfrac{\partial N_x(y_N)}{\partial \hat{y}_N} \end{vmatrix}.$$

(5.29)

The state filtering error, $\tilde{y}(\underline{x}, k+1|k+1)$, given by Eqn. (30), is comprised of the state prediction error, $\tilde{y}(\underline{x}, k+1|k)$, as adjusted by a filtering term, which is the product of the filtering gain, K, and the innovation error, v.

$$\tilde{y}(\underline{x}, k+1|k+1) = \tilde{y}(\underline{x}, k+1|k) - K(\underline{x}, k+1) \times v(k+1).$$

(5.30)

The initial state estimation error, $\tilde{y}(\underline{x}, k|k)$, is set to be zero.

$$\tilde{y}(\underline{x}, k|k)\big|_{k=0} = 0.$$

(5.31)

The one-step-ahead prediction error covariance matrix, M, is approximated, which reduces the required calculations. It utilizes the previous calculation of the prediction error covariance and adjusts it by a literal interpretation of the error covariance using the product of the prediction errors.

$$E\left[\left(y(k+1) - \hat{y}(k+1|k)\right)\left(y(k+1) - \hat{y}(k+1|k)\right)^T\right] = E\left[\tilde{y}(k+1|k)\tilde{y}(k+1|k)^T\right] = M.$$

(5.32)

Since this filtering algorithm converts the system being analyzed from a distributed to a lumped-parameter-type model, and thereby reduces the spatial cross-correlation of the prediction errors, a "sliding-mean" (to be described later) is utilized to incorporate neighboring prediction errors in the calculation of each prediction error.

$$M(\underline{x}, \underline{x}', k+1|k) = M(\underline{x}, \underline{x}', k|k-1)$$
$$+ \gamma(k)\left\{\left(\tfrac{1}{S_x \times S_{x'}}\right)_{\Omega_x} \int_{\Omega_{x'}} \delta y(\underline{x}, k+1|k) \times \delta y^T(\underline{x}', k+1|k) \times d\Omega d\Omega' - M(\underline{x}, \underline{x}', k|k-1)\right\},$$

(5.33)

where S_x and $S_{x'}$ are the correlation intervals around x and x', respectively, and $\gamma(k) = \frac{1}{k+2}$

The initial value of the prediction error covariance matrix is set to a value somewhat dependent on the model being analyzed, though it should be set to a value larger than the expected steady-state value,

48

$$M(\underline{x},\underline{x}',k|k-1)\big]_{k=1} = M_0(\underline{x},\underline{x}').\qquad\qquad (5.34)$$

These equations have been assembled in a MATLAB based code.

The time averaging factor, $\gamma(k) = \frac{1}{k+2}$, was chosen specific to the iteration initialization of the algorithm code. Since $k = 0$ on the first pass through the calculation of M from Eqn. (33), $\gamma(k)|_{k=0}$ is initially equal to $\frac{1}{2}$, and the first calculated value of M is equal to the average of M_0 and the integral term.

The purpose of the jacobian matrix used in Eqn. (28), and expanded in Eqn. (29), is to take the amount of change predicted for the states (contaminant concentrations) over the next iteration and apply that proportionally to other variables related to those states, such as the state estimation error $\tilde{y}(\underline{x}, k|k)$, to obtain predicted values of those variables.

The portion of the state estimation algorithm which sets this method apart from other state estimation algorithms is the estimation of the prediction error covariance matrix, as given by Eqn. (33). The approximation of M incorporates a "sliding mean" into the calculations. A sliding-mean across the space coordinates is used to calculate the individual elements within the prediction error covariance matrix so as to partially reintroduce the spatial correlation component of the covariance matrix back into the filtering calculations, which were removed from the calculations when the system was "lumped" into discrete points. The sliding mean used in this case is a spatially moving average of neighboring state prediction errors, encompassing spatially adjacent neighboring points from the physical habitat being analyzed. The estimated sample prediction error covariances within the range of the sliding mean are added together then averaged.

5.7   Korbicz suboptimal sensor location algorithm

The following equations for the Suboptimal Sensor Location algorithm take the original suboptimal filtering equations and incorporates a switching variable, λ, which denotes whether or not a possible sensor location in the Euclidian space actually has a sensor, as determined from the proposed sensor configuration being investigated at that time (J. Korbicz, 1991). λ is specified at each possible sensor location, with a value of 1 if a sensor

is present, or a value of 0 if no sensor is present in that location. The discrete adjoint (costate) variables are then calculated from the associated Hamilton function. The filtering and adjoint variables are used to calculate a switching function, which determines the new values of λ (new sensor locations).

The revised filtering equations are approximately (only presenting those equations which have changed and neglecting some unnecessary subscripts),

$$z(x,k) = \left[z(x_1,k), z(x_2,k), \ldots, Z(x_N,k)\right]^{\mathrm{T}} = \lambda_{j,k} \left[N_{\mathrm{H}}(y,x_j,k) + v(x_j,k)\right] \quad j = 1,2,\ldots,N.$$

$$(5.35)$$

The new measurement vector is the same as before, except that each possible sensor location (from the N locations) lacking a sensor (at time k) has a value of λ equal to zero, so no signal comes from that location. Mathematically, the constraint that only N' sensors can be placed in the N locations can be stated as,

$$\sum_{j=1}^{N} \lambda_{j,k} = N', \quad \lambda_{j,k} = 0 \ or \ 1.$$

$$(5.36)$$

For our space habitat example, we have added the constraint that a maximum of one sensor can be placed at any possible location.

The prior adjustment to the state estimate formed by the product of the filter gain matrix and the innovation error in Eqns. (22) and (30) have been transformed into more complex equations due to the addition of the sensor switching variable for each possible location, λ.

$$\hat{y}(x,k+1|k+1) = N_x(\hat{y},x,k|k) + G(x,k+1|k),$$

$$(5.37)$$

$$\tilde{y}(x,k+1|k+1) = \tilde{y}(x,k+1|k) - G(x,k+1|k),$$

$$(5.38)$$

$$G(x,k+1|k) = \sum_{i=1}^{N'} \sum_{j=1}^{N'} M(x,x_i,k+1|k) \times \left(N_H(y,x_i,k|k)\right)_{\hat{y}} \times \lambda_{i,k+1} \times \Gamma^{-1}(x_j,x_i,k+1|k)$$

$$\times \left[z(x_j,k+1) - \lambda_{j,k+1} \times N_H(y,x_j,k+1|k)\right]. \qquad (5.39)$$

The variables are,

$\lambda_{j,k} = 1$, if a sensor is located at the point x_j at time k; 0, otherwise.

N' = number of sensors.

N = number of possible sensor locations $(N^3 \, N')$.

N_H = vector function at the measurement points, non-linear function of states.

$(N_H)_{\hat{y}}$ = gradients of state updates (Jacobian matrix).

The scalar performance functional, J (in continuous form), to be minimized for the sensor location portion of the algorithm is the integral of the cost function, $\Im$, which has been selected to be the trace of the prediction error covariance matrix,

$$J = \int_{t_0}^{t_K} \Im(Y,u,t)dt = \int_{0}^{t_K} tr\left[M(x,x',t)\right]dt . \qquad (5.40)$$

This minimization seeks the reduction of the prediction error over the period of time being analyzed. The trace of the prediction error covariance matrix is the sum of the squares of each state's prediction error. This captures the largest values in the matrix, and yields a positive value for each. Minimizing the trace reduces the error between the predicted states and the actual states, and places the sensors at the locations which are associated with the least overall system state estimation error.

The scalar Hamilton function of the system, H (in continuous form), is the sum of the cost function, $\Im$, and the product of the adjoint variables, ϕ, ψ, θ, times the right hand side of the suboptimal filtering equations (the discrete forms are given by Eqns. (22), (30), and (33)). The Hamiltonian in continuous form is,

$$H(M,\hat{y},\tilde{y},\phi,\psi,\theta) = \mathrm{tr}[M(\underline{x},\underline{x}',t)] + \phi^{\mathrm{T}}(\underline{x},t) \times \frac{\partial \hat{y}(\underline{x},t)}{\partial t} + \psi^{\mathrm{T}}(\underline{x},t) \times \frac{\partial \tilde{y}(\underline{x},t)}{\partial t}$$

$$+ \mathrm{tr}\left[\theta^{\mathrm{T}}(\underline{x},\underline{x}',t) \times \frac{\partial M(\underline{x},\underline{x}',t)}{\partial t}\right]. \tag{5.41}$$

The corresponding adjoint variable equations as calculated by Korbicz are,

$$\phi(\underline{x},k|k) = -\frac{\partial H(\cdot)}{\partial \hat{y}(\cdot)}$$

$$= -(\mathrm{N}_{\mathrm{x}})_{\hat{y}}^{\mathrm{T}} \times \phi(\underline{x},k+1|k+1) + \sum_{i=1}^{N'}\sum_{j=1}^{N'}\left(\mathrm{N}_{\mathrm{H}}(\hat{y},\underline{x}_j,k+1|k)\right)_{\hat{y}}^{\mathrm{T}} \times \lambda_{j,k+1}$$

$$\times \Gamma^{-1}(\underline{x}_j,\underline{x}_i,k+1|k) \times \lambda_{i,k+1} \times \left(\mathrm{N}_{\mathrm{H}}(\hat{y},\underline{x}_i,k+1|k)\right)_{\hat{y}}$$

$$\times M^{\mathrm{T}}(\underline{x},\underline{x}_i,k+1|k) \times \left[\psi(\underline{x},k+1|k+1) - \phi(\underline{x},k+1|k+1)\right], \tag{5.42}$$

$$\psi(\underline{x},k|k) = -\frac{\partial H(\cdot)}{\partial \tilde{y}(\cdot)}$$

$$= -(\mathrm{N}_{\mathrm{x}})_{\tilde{y}}^{\mathrm{T}} \times \psi(\underline{x},k+1|k+1)$$

$$- \frac{2}{S_x \times S_{x'}} \times \theta(\underline{x},\underline{x},k+1|k+1) \times \int_{\Omega_{x'}} \tilde{y}(\underline{x}',k|k)d\underline{x}', \tag{5.43}$$

$$\theta(\underline{x},\underline{x}',k) = -\frac{\partial H(\cdot)}{\partial M(\cdot)}$$

$$= -I + \gamma(k) \times \theta(\underline{x},\underline{x}',k+1)$$

$$+ \sum_{i=1}^{N'}\sum_{j=1}^{N'}\left[\xi(\underline{x}_j(k+1),k+1) - \lambda_{j,k+1} \times \mathrm{N}_{\mathrm{H}}(\hat{y},\underline{x}'_j(k+1),k+1|k)\right]^{\mathrm{T}}$$

$$\times \Gamma^{-1}(\underline{x}_j(k+1),\underline{x}'_i(k+1),k+1|k) \times \lambda_{i,k+1} \times \left(\mathrm{N}_{\mathrm{H}}(\hat{y},\underline{x}'_i(k+1),k+1|k)\right)_{\hat{y}}$$

$$\times \left[\psi(\underline{x},k+1) - \phi(\underline{x},k+1)\right] \times I, \tag{5.44}$$

with initial conditions,

$$\phi(\underline{x},k)_{k=K} = 0, \tag{5.45}$$

$$\psi(\underline{x},k)_{k=K} = 0, \tag{5.46}$$

52

$$\theta(x, x', k)_{k=K} = 0, \qquad (5.47)$$

where,

ϕ, ψ, θ = adjoint variables,

tr[•]= trace of a matrix (sum of the main diagonal), and

K = final iteration count.

The above adjoint variable equations are integrated backwards from the ending time $k = K$ to $k = 1$, calculating the switching function ε_{jk} for each point. The switching function as calculated by Korbicz (J. Korbicz, 1991), is derived from the portion of the Hamiltonian of Eqn. (67) that is linear with respect to λ. The switching function as calculated by Korbicz is as follows,

$$\varepsilon_{jk} = E\left[\int_\Omega \left[\phi^{*T}(x, k+1|k+1) - \psi^{*T}(x, k+1|k+1)\right]\right.$$
$$\times M^*\left(x, x'_j(k+1), k+1|k\right) \times \left(N_H\left(y, x'_j(k+1), k+1|k\right)\right)_{\hat{y}} \times \Gamma^{-1}\left(x'_j(k), k+1|k\right)$$
$$\times \left.\left[z\left(x'_j(k+1), k+1\right) - N_H\left(\hat{y}^*, x'_j(k+1), k+1|k\right)\right]\right] \quad j = 1, 2, \ldots, N, \ k = 1, 2, \ldots, K .$$

$$(5.48)$$

The switching function values, ε_{jk}, are averaged over time (due to the E[•] term) for each point. The summed values are then ordered from maximum to minimum, in the order of the best estimated locations for the sensors. The N locations which have the largest values of ε_j are then considered to be the best locations given the restrictions on the number of allowable sensors (for that run). These are the sensor locations to be set ($\lambda_j = 1$) in the next iteration run; sensors will be placed in those locations.

The optimal sensor locations are updated after each run until no further improvements are apparent, as judged from the trace of the prediction error covariance matrix. It is then decided whether the optimized sensor configuration will yield sufficiently accurate results for the contaminant scenario. Korbicz states that the trace of the prediction error covariance matrix can be used for this. Another measure of the accuracy of the sensor

53

configuration is the average error between the estimated states and the actual states. This average state error measure was used by the author in this study, as it gives a better estimate of the errors that will be produced by the filtering algorithm.

If the optimized sensor configuration does not yield sufficiently accurate results, then the number of sensors used in the configuration is increased after each run until the desired accuracy is achieved. If the optimized sensor configuration does yield sufficiently accurate results, then the number of sensors used in the configuration is decreased until no more sensors can be removed without causing the configuration to fail the accuracy test. The resulting number of sensors and locations of these sensors are considered to then be the best estimate of the minimum number of sensors which will achieve the desired average accuracy averaged over all selected locations.

Korbicz's algorithm formulation does not contain any existence theorem showing that the approximations so arrived at converge to a solution which is globally minimal. The filtering portion of the algorithm relies on a variation of the Kalman Filter theorems, but the sensor location portion of the algorithm is a derivation using control theory principles, and is demonstrated in an example in Korbicz's papers.

5.8   Suboptimal filtering and sensor location results

Using the previously specified contaminant concentration scenario, variations of sensor configurations containing sensors placed at spatial locations x_1, x_6, x_{11} were then applied and analyzed using the suboptimal filtering and sensor location algorithm. A step input was introduced into the simulations at spatial location x_{11} at time 0.01 sec. The simulations were run for simulated durations of 2 seconds, which was enough time for the states to progress to near-equilibrium (the spatial locations were close together). Testing was performed to establish the appropriate simulation time step and other algorithm parameters which can be varied. The time step increment was started at the stability threshold and reduced until the simulation results did not appreciably change; the time step finally selected was 0.003 sec. The other parameter selections and variations are described in the next section.

The suboptimal algorithm is designed to assess the state prediction error of a number of sensors in a particular configuration under investigation, perform comparisons between configurations of sensors, and place those sensors in optimal locations. When three sensors for three locations are being assessed, only one configuration is possible. When the use of two sensors is being assessed for three possible sensor locations, three different sensor configurations are possible, and the algorithm should indicate the best two locations for those sensors, as will be shown below.

Sensor configurations were tested with sensors placed at each possible location and then placed in groups of two. A full configuration consisted of the placement of sensors at each of the three possible spatial locations (x_1, x_6, x_{11}). In the terminology of switching sensors on and off (1 or 0), this full configuration would be $\lambda = [1\ 1\ 1]$, since a sensor is placed at each possible spatial location which can accept a sensor. The placement of sensors only at locations x_1 and x_6 translates to $\lambda = [1\ 1\ 0]$. For each sensor configuration, correlation neighborhoods of $\Delta n = 0, 1, 2, 3, 4, 5, 11$ were run. The average state error was calculated for each run. A summary of the results for $\Delta n = 4$ is shown in Table 2. Plots of the actual system states, sensor measurements, and the estimated system states for $\Delta n = 4$ and sensors at locations x_6 and x_{11}, are shown in Figure 4.

Table 2. Results of Korbicz Suboptimal Filter and Sensor Location Algorithm

Sensor Placement $\lambda = \left[\lambda_{(x_1)}\ \lambda_{(x_6)}\ \lambda_{(x_{11})} \right]$	Correlation Neighbors Δn	Average State Error	Prioritized Sensor Locations
[1 1 1]	4	0.01108	[11 6 1]
[1 1 0]	4	0.04481	[6 11 1]
[1 0 1]	4	0.01460	[11 6 1]
[0 1 1]	4	0.01103	[11 6 1]

states, measurements (...), and estimated (– –) states (x1, x6, x11),

Nsensors = 2 –> [6 11] , nbr = 4 , korbicz.m
Qi = 0.0016, Ri = 0.0025
trace P = 0.005972 , ave. error = 0.01103
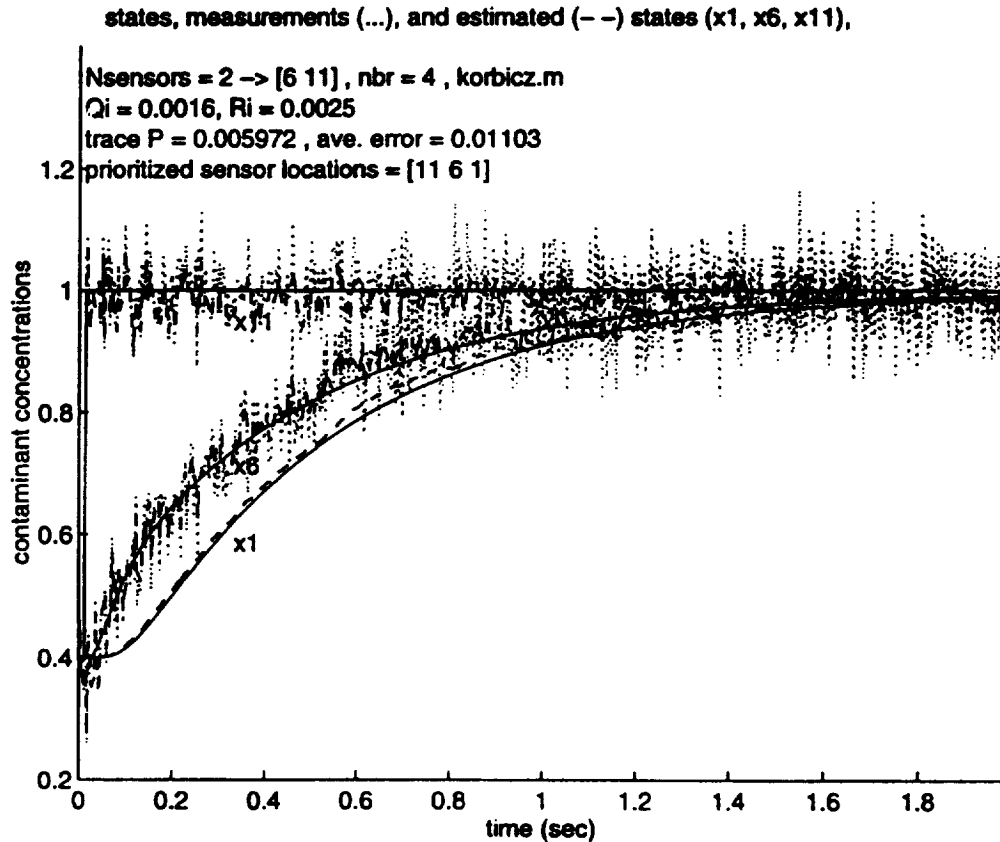prioritized sensor locations = [11 6 1]

Figure 4. Korbicz Suboptimal Filter & Estimate of States, Sensors at x_6 and x_{11},
Response to a Step Input at Location x_{11}, $\Delta n = 4$

When sensors were placed at locations x_6 and x_{11}, and using $\Delta n = 4$, the average state error over the 2.0 sec. duration of the simulation was calculated to be 0.0110, slightly less than that calculated for the Extended Kalman Filter using the same sensor configuration (previously 0.01199). The prioritized sensor locations calculated by the suboptimal sensor placement algorithm was [11 6 1], which means that the algorithm indicates that the best locations for two sensors for this step input scenario is in locations x_{11} & x_6. As shown by the results from the Extended Kalman Filter tests, these are probably the best locations. Placing sensors at spatial locations x_1 & x_{11} yielded a significantly greater average state error of 0.0146.

If the simulation started off placing sensors at locations x_1 & x_6, using $\mathcal{E}n = 4$, the resulting sensor location priority would indicate that placing sensors at x_6 & x_{11} would

yield better results. Even though the pair of locations $\underline{x}_1$ & $\underline{x}_{11}$ yields better estimates of the concentrations when using Korbicz's Suboptimal Filtering algorithm, the pair of locations $\underline{x}_6$ & $\underline{x}_{11}$ are the ones that actually yield the best concentration estimation results, since the Extended Kalman Filter is the likely Filter to be used in the space habitat.

5.9 Sensor location algorithm discussion

There is a large variation in the algorithm selected prioritized sensors for correlation neighborhoods $\Delta n = 0 - 32$. There are two main reasons for this, corresponding to two mistakes in the formulation of the adjoint equations. The first mistake is in the sign of the adjoint equations. The equations to calculate an adjoint variables, as derived in (W.F. Ramirez, 1994), are,

$$\phi(x, k|k) = +\frac{\partial H(\cdot)}{\partial \hat{y}(\cdot)},$$

(5.49)

$$\psi(x, k|k) = +\frac{\partial H(\cdot)}{\partial \tilde{y}(\cdot)},$$

(5.50)

$$\theta(x, x', k|k) = +\frac{\partial H(\cdot)}{\partial M(\cdot)}.$$

(5.51)

The corresponding Korbicz algorithm equations, as presented in Eqns. (42), (43), & (44), are of the opposite signs. Korbicz seems to have taken the calculations of the continuous-time adjoint variables from (J. Korbicz et al., 1988), and to have simply called them discrete-time (J. Korbicz, 1991). This sign reversal has two primary effects in the calculation of the adjoint variables: 1) the adjoint equations have significant terms which oscillate between negative and positive values, and 2) the Hamiltonian has to be maximized. The first point is easy to see. For example, in Eqn. (43), if we assume that $\tilde{y}(\underline{x}', k|k)$ is a very small value, and that the $(N_x)_{\tilde{y}}^T$ term is positive-definite such as in our simulation, then Eqn. (43) simply changes the sign of $\psi(\underline{x}, k|k)$. This also occurs for the calculation of $\phi(\underline{x}, k|k)$.

57

This sign reversal also forces Korbicz to try to maximize the Hamiltonian, when it should actually be minimized because we want to minimize the cost functional. At one iteration, the values of the λ-dependent portion of the Hamiltonian could indicate that the sensor location priority is one particular order, and due to the sign reversals, the very next iteration will indicate that the sensor location priority is of the opposite order. The values of ε_j bounce between extremes as the adjoints are calculated.

The second mistake is in the calculation of the adjoint equations. It seems that Korbicz was not rigorous in his calculations; the use of the $(\cdot)$ placeholder in the denominators of Eqn. (42), (43), & (44) ignores some complex subscript problems. In examining Eqns. (37), (39), & (33), we see that $\hat{y}$ is a function of G, which is a function of M (different time index from $M(\cdot)$), which is a function of $\tilde{y}$. Since $\hat{y}$ is therefore a function of $\tilde{y}$ down the line, then it would follow that there should be a $\phi(\underline{x}, k|k)$ in Eqn. (43) since the Hamiltonian H contains $\phi(\underline{x}, k|k) \times \hat{y}$.

In addition, the calculation of $\theta(\underline{x}, \underline{x}', k|k)$ seems to be oversimplified, if Korbicz's equation is taken literally (it can result in $\theta(\underline{x}, \underline{x}', k|k)$ being diagonal, with all of the terms being the same). It is therefore surprising that the calculation of the correct sensor location priority actually returns correct values, though only for large correlation neighborhoods.

5.10 Conclusions

Once the parameters are set correctly, the Korbicz Suboptimal Filter estimates the concentrations of the contaminants (states) as well as the Extended Kalman Filter, for the contamination scenario tested in this paper.

The Sensor Location Algorithm does not work properly until the correlation neighborhood reaches some value, though this value is not presently able to be determined beforehand. Once that value is achieved, though, the Suboptimal Filter portion may imply that one particular sensor configuration is optimal (through examining the average state error), while the Sensor Location Algorithm may select a different sensor configuration as optimal (which coincided with the Extended Kalman Filter results in our example).

58

The calculation of the adjoint equations in the Sensor Location Algorithm is suspect; some terms may have been left out or approximated, though this is not mentioned by Korbicz. It was necessary to re-derive all of Korbicz's equations to determine the correct equation multiplications, since the subscripted equations presented by Korbicz in his papers are extremely confusing. When this re-derivation was performed, some neglected terms were discovered. Before the Algorithm can be used with more confidence, the significance of those missing terms needs to be evaluated. Until then, use this algorithm with caution.

The general methodology developed by Korbicz looks promising, but the sensor placement algorithm equations presented by Korbicz are not rigorous, and they leave a significant amount of variation in their application. We shall be recalculating the algorithm equations in an attempt to obtain more consistant results.

Chapter 6

Conclusions

To date we have developed two and three dimensional distributed parameter models of contaminant transport, developed a new Implicit Kalman Filtering approach for contaminant identification, and developed a suboptimal sensor placement algorithm. This coming year we plan to work on a contaminant source diagnosis problem, develop a three dimensional contaminant visualization program, use the Implicit Kalman Filter to estimate three dimensional contaminant concentration profile, and develop an optimal sensor placement algorithm.

References

BERGLUND, B., GRIMSRUD, D. T., AND SEIFERT, B., 1989, Special Issue on Indoor Air Quality. *Environment International,* **15,** Numbers 1–6.

BERGLUND, B., BERGLUND, U., LINDVALL, T., SEIFERT, B., AND SUNDALL, J., 1986, Special Issue on Indoor Air Quality. *Environment International,* **12,** Numbers 1–4.

BERRY, C., AND BRACKBENBURY, A., 1991, On-line Gas Analysis. *Measurement & Control,* **24,** 231–236.

BIERMAN, G. J., 1977 *Factorization Methods for Discrete Sequential Estimation.* New York: Academic Press.

BIRD, R. B., STEWARD, W. E., AND LIGHTFOOT, E. N., 1960, *Transport Phenomena.* New York: John Wiley.

COLEMAN, M. E., AND JAMES, J. T., 1994, Airborne Toxic Hazards. In: Nicogossian, A. E., Huntoon, C. L., and Pool, S. L., (eds). *Space Biology and Medicine.* Philadelphia: Lea and Febiger, 141–156.

COVAULT, C., 1983, Explosion and leak cripples Salyut-7 effort. *Aviation Week & Space Technology,* October 10, 1983, 23-26.

ECLSS INTEGRATION ANALYSIS, 1990, Computer Aided System Engineering and Analysis (CASE/A) User's Manual. Version 4.1. McDonnell Douglas Space Systems Company, Huntsville Division, October 1990.

EVERITT, B.S. AND GRAHAM, D., 1992, *Applied Multivariate Data Analysis*, Oxford University Press, New York, QA278.E89.

GODISH, T., 1995, *Sick Buildings. Definition, Diagnosis and Mitigation*. Boca Raton: CRC Press.

GOLUB, G. H., AND VAN LOAN, C. F., 1989, *Matrix Computations*. 2nd edition. Baltimore: John Hopkins University Press.

JAMES, J. T., AND COLEMAN, M. E., 1994, Toxicology of Airborne Gaseous and Particulate Contaminants in Space Habitat. In: Sulzman, F. M., and Genin, A. M., (eds). *Life Support and Habitability*. Washington: American Institute of Aeronautics and Astronautics, 37–60.

JAMES, J. T., LIMERO, T. F., LEANO, H. J., BOYD, J. F., AND COVINGTON, PH. A., 1994, Volatile Organic Contaminants Found in the Habitable Environment of the Space Shuttle: STS–26 to STS–55. *Aviation, Space and Environmental Medicine*, **65**, 851–857.

KOCACHE, R., 1994, Gas Sensors. *Sensor Review*, **14**, 8–12.

KORBICZ, J., 1986, Suboptimal State Estimation Algorithm for Non–Linear Discrete–Time Distributed–Parameter Systems. *Int. J. Sys. Sci.*, **17**(5), 725–734.

KORBICZ, J., 1991, Discrete–Scanning Observation Problem for Stochastic Non–Linear Discrete–Time Distributed–Parameter Systems. *Int. J. Sys. Sci.*, **22**(9), 1647–1662.

KORBICZ, J., ZGUROVSKY, M. Z., AND NOVIKOV, A. N., 1988, Suboptimal Sensors Location in the State Estimation Problem for Stochastic Non–Linear Distributed Parameter Systems. *Int. J. Sys. Sci.*, **29**(9), 1871–1882.

KUBRUSLY, C. S., 1977, Distributed Parameter Systems Identification – A Survey. *International Journal of Control*, **26**, 509–535.

LOGAN, J. S., 1989, Health Maintenance on Space Station. In: Lorr, D. B., Garshnek, and V., Cladoux, C., (eds). *Working in Orbit and Beyond: The Challenges for Space Medicine.* Science and Technology Series, **72**, 87–99. San Diego: American Astronautical Society.

MAGNUS, J. R. AND NEUDECKER, H., 1988, *Matrix Differential Calculuc with Applications in Statistics and Econometrics.* John Wiley & Sons, Chichester, QA188.M345.

MATHWORKS, 1995, it MATLAB. The MathWorks, Inc., Natick, MA.

MØLHAVE, L., 1989, The Sick Building and Other Buildings with Indoor Climate Problems. *Environment International,* **15**, 65–74.

MØLHAVE, L., BACH, B., AND PEDERSEN, O. F., 1986, Human Reactions to Low Concentrations of Volatile Organic Compounds. *Environment International,* **12**, 167-175.

NATIONAL ACADEMY OF SCIENCES, 1981, *Indoor Pollutants.* Washington: National Academy Press.

NATIONAL AERONAUTICS AND SPACE ADMINISTRATION, 1989, *Airborne Particle Measurement in the Space Shuttle.* NASA.

NATIONAL RESEARCH COUNCIL COMMITTEE ON TOXICOLOGY, 1994, *Spacecraft Maximum Allowable Concentrations.* Washington: National Academy Press.

NATIONAL RESEARCH COUNCIL COMMITTEE ON TOXICOLOGY, 1992, *Guidelines for Developing Spacecraft Maximum Allowable Concentrations for Space Station Contaminants.* Washington: National Academy Press.

OZKAYNAK, H., RYAN, P. B., ALLEN, G. A., AND TURNER, W. A., 1982, Indoor air quality modeling: compartmental Approach with Reactive Chemistry. *Environment International,* **8**, 461-471.

PERRY, J. L., 1993, *Computerized atmospheric trace contaminant control simulation for manned spacecraft*. NASA TM-108409, George C. Marshall Space Flight Center, Alabama.

PETO, P. G., 1981, Results of Soviet-Hungarian Space Research. *East European Report*, No. 699, 4-12, April 3, 1981.

PRESS, W. H., FLANNERY, B. P., TEUKOLSKY, S. A., AND VETTERLING, W. T., 1989, *Numerical Recipes – The Art of Scientific Computing*. Cambridge University Press, Cambridge, QA297.N866.

RAMIREZ, W. F., 1994, *Process Control and Identification*. Academic Press, Inc., Boston, TS156.8.R36.

RAY, W. H., AND LAINIOTIS, D. G., 1978, *Distributed Parameter Systems: Identification, Estimation and Control*.New York: Marcel Dekker.

RYAN, P. B., SPENGLER, J. D., AND HALFPENNY, P. F., 1988, Sequential Box Models for Indoor Air Quality: Application to Airliner Cabin Air Quality. *Atmospheric Environment*, **22**, 1031-1038.

SAVINA, V. P., Unpublished date. Provided by Dr. John T. James, NASA/Johnson Space Center.

SKLIAR, M., AND RAMIREZ, W. F., 1996, Square root implicit Kalman filtering. *Proceedings of the 13th IFAC World Congress*, San Francisco, California.

SKLIAR, M., AND RAMIREZ, W. F., 1995a, Kalman Filter for Discrete Implicit Systems, *Proc. 1995 American Control Conference*, Seattle, Washington, 524-528.

SKLIAR, M., AND RAMIREZ, W. F., 1995b, Implicit Kalman Filtering, submitted to *International Journal of Control*.

SMITH, G. J., 1995, *Sensor Configuration Observability for a Simplified Contaminant Transport Simulation*. Tech Note #30, NSCORT/CSEH internal document, University of Colorado Aerospace Engineering Department.

SON C., AND BARKER, R. S., 1993, U.S. Lab-A Module Cabin Air Distribution in Space Station. *Proc. 23rd International Conference on Environmental Systems*, Colorado Springs, Colorado.

TODD, P., SKLIAR, M., RAMIREZ, F., SMITH, G., MORGENTHALER, G., MCKINON, J., OBERDÖERSTER, G., AND SCHULZ, J., 1994, Inhalation Risk in Low-gravity Spacecraft. *Acta Astronautica*, **33**, 304-315.

TODD, P., SKLIAR, M., SMITH, G., RAMIREZ, F., OBERDÖERSTER, G., AND MORGENTHALER, G., 1993, Physics, Chemistry and Risk of Thermodegradation in Long-Mission Space Flight, *Proc. 23rd International Conference on Environmental Systems*, Colorado Springs, Colorado.

TZAFESTAS, S. G.,(ED.) 1982, *Distributed Parameter Control Systems*. Oxford: Pergamon Press.

WALPOLE, R. E. AND MYERS, R. H., 1985, *Probability and Statistics for Engineers and Scientists*. Macmillan Publishing Company, New York, TA340.W35.

WHITE, R. J., AND LUJAN, B. F., 1989, Current Status and Future Direction of NASA's Space Life Sciences Program. In: Lorr, D. B., Garshnek, and V., Cladoux, C., (eds). *Working in Orbit and Beyond: The Challenges for Space Medicine*. Science and Technology Series, **72**, 1–7. San Diego: American Astronautical Society.